EFFECT OF AMBIENT DURING ANNEALING ON ELECTRICAL PROPERTIES OF SOL-GEL DERIVED LEAD ZIRCONATE TITANATE (PZT) THIN FILMS

by

NAYAN KUMAR PUTHAL

MATERIALS SCIENCE PROGRAMME

INDIAN INSTITUTE OF TECHNOLOGY KANPUR

MARCH, 1997

EFFECT OF AMBIENT DURING ANNEALING ON ELECTRICAL PROPERTIES OF SOL-GEL DERIVED LEAD ZIRCONATE TITANATE (PZT) THIN FILMS

A Thesis submitted
in Partial Fulfilment of the Requirement
for the Degree of
MASTER OF TECHNOLOGY

by
NAYAN KUMAR PUTHAL.

to the
MATERIALS SCIENCE PROGRAMME
INDIAN INSTITUTE OF TECHNOLOGY, KANPUR

Mach 1997

MSP-1997-M-PUT-PUFF

To

My

Parents

CERTIFICATE

This is to certify that the work presented in this thesis entitled, " EFFECT OF AMBIENT DURING ANNEALING ON ELECTRICAL PROPERTIES OF SOL-GEL DERIVED LEAD ZIRCONATE TITANATE (PZT) THIN FILMS " by **Nayan Kumar Puthal** is a record of work carried out under our supervision and is not been submitted elsewhere for a degree.

(D.C. Agrawal)
Materials Science Programme
Indian Institute of Technology
Kanpur,India

(Y.N. Mohapatra)
Materials Science Programme
Indian Institute of Technology
Kanpur,India.

March, 1997.

ABSTRACT

Thin films of ferroelectric lead zirconate titanate (PZT) have many potential applications including that of non-volatile random access memory in computer systems. However, there are at present several problems relating to the electrical properties of these films such as fatigue, depolarization and imprint which are not well understood. There have been few reports on the effect of ambient during annealing on the electrical properties of the films. In this work the properties of nitrogen annealed films are studied and compared with oxygen annealed films to evaluate the role of combination of ambient during annealing and heating schedules on the electrical properties viz. dc leakage current, hysteresis loop parameters and depolarization characteristics. Special emphasis is given to depolarization study of the films.

The films of composition $Pb_{1.05}(Zr_{0.53}Ti_{0.47})O_3$ in the thickness range 1.7-1.78μm been prepared using sol-gel technique on Pt substrates. For studying the effect of ambient on final stage of annealing two different heat treatment sequence was used. In all samples nitrogen was used as the ambient on the final stage of annealing. Samples fired at 400 ^{0}C during intermediate stage and annealed at 700 ^{0}C are termed as LIRF samples and those fired at 600 ^{0}C and annealed at 700 ^{0}C are termed as HIRF samples. Routine characterization of samples have been carried out using Double Beam Spectrophotometry, XRD, I-V, and P-E hysteresis measurements. The depolarization behaviour of the films have been studied using a new measurement sequence in which the loss of remnant polarization is monitored in time domain after preparing the polarization state of the sample by a square voltage pulse.

Perovskite phase was obtained for all the samples studied. However, peaks in the spectra for LIRF (N_2) are broader than those for LIRF (O_2) which indicates that perovskite phase formation is slower in nitrogen ambient than oxygen ambient. Again the peaks of LIRF (6hr N_2) are sharper than LIRF (1hr N_2) samples. With increase in annealing time, peaks corresponding to perovskite phase becomes progressively sharper. However for samples fired at high intermediate temperature, ambient has no significant effect on phase formation.

The samples annealed in nitrogen ambient have significantly higher remnant polarization and lower coercive field than those annealed in oxygen. This improvement in ferroelectric parameter

attributed to presence of oxygen vacancies which make domain movement easier. For nitrogen ambient annealing, sample fired at low intermediate temperature have larger leakage current than its oxygen annealed counterpart. On the other hand keeping the heating schedule same as HIRF, oxygen ambient annealed sample have higher leakage current. Both the observations are consistent with the fact that concentration of free charged oxygen vacancies control conductivity. When lead vacancies and oxygen vacancies are in large concentration, the leakage current gets reduced due to pair formation between lead and oxygen vacancies. All nitrogen annealed samples have poor fatigue characteristics due to presence of large number of oxygen vacancies. During depolarization measurements in LIRF(N_2) samples there is a strong correlation between the final polarization state achieved and the final internal bias. If the final polarization state achieved is $+P_r$ then internal bias is negative and vice versa. Whereas for HIRF(N_2) sample, the internal bias is found to be always negative indicating that positive polarization state is the preferred stable state. The polarization loss percent in LIRF(N_2) samples are lower than LIRF(O_2) samples. This correlates with the occurrence of lower internal bias in LIRF(N_2) samples than LIRF(O_2) samples. Polarization loss is found to be smaller in all cases of nitrogen annealed samples except for HIRF (N_2) samples. For HIRF (N_2) samples, polarization loss is found to be high only when the polarization state is switched from positive remnant polarization to negative remnant polarization. This observation provides proof of the fact that internal bias is responsible for depolarization.

The experimental observations are correlated with processing conditions through a comparison of measured properties for different combinations of ambient and heating schedule. It is found that nitrogen annealing ambient, leads to large concentration of oxygen vacancies which in turn leads to larger leakage current, easier domain switching, and poorer fatigue resistance. It is concluded that annealing under oxygen ambient and at high temperature favour formation of lead vacancies. These lead vacancies tend to form defect dipoles or associates with oxygen vacancies leading to removal of charged oxygen vacancies. The presence of these defects seem to be responsible for lowering conductivity, and act as a source of internal bias and depolarization.

Acknowledgments

I wish to express my deep sense of gratitude to my thesis supervisors Dr. D. C. Agrawal and Dr. Y. N. Mohapatra for having given me a free rein in the formulation and implementation of the research work, and for their expert guidance which helped me be on the right track.

I am extremely grateful to Dr. Jitendra Kumar for allowing me to have free access to all the facilities for I-V and thickness measurements.

I wish to acknowledge my appreciation to my labmate Subashish who developed the technique for film preparation and for his useful suggestions and cooperation in sorting out many problems in my entire work. I wish to thank him for his encouraging words and brotherly advice which are motivating.

I wish to thanks my lab seniors Atanu, Ajay , Ramesh and Archanaji for their care which they had taken towards me. Special thanks are due to other labmates Gurvinder, Monaj, Sarvesh, Pankaj, Bhaumik and Souman for their ever smiling faces. A word of thanks to my other dept. friends Senapathy, Rajnish, Rajesh, Lakhmani, Pragya, and M.K. Singh for their help and cooperation throughout my M.Tech. program. I also express my sincere thanks to all the staff and members of MSP and ACMS for their help and cooperation towards me.

I sincerely appreciate the companionship of all my Oriya friends who made my staying here really charming and worthwhile. My interaction with them academic and otherwise, has always been fruitful and pleasant.

Last but not least, I thank my family member for their constant source of encouragement through out this thesis work.

Contents

List of Figures

List of Tables

Chapter 1

Introduction

Ferroelectricity, the reversal of spontaneous polarization by the applied electric field, was first discovered by Valasek in Rochelle salt (Sodium potassium tartrate) in 1923. After this discovery, ferroelectricity was reported in many more crystals like KDP (Potassium dihydrogen phosphate), ADP (Ammonium dihydrogen phosphate) etc. But, significant breakthrough in understanding the structural origin of ferroelectricity came through the discovery of the same in $BaTiO_3$ ceramics in 1945. The large dielectric and piezoelectric constants of these materials immediately made them attractive candidates for variety of applications. For many years, ferroelectrics dominated the field of sonar detectors, phonograph pickups and so on. Pyroelectric properties of these materials are utilized in fabrication of devices such as IR detectors etc. However none of these devices directly utilized the ferroelectric nature of the material, namely large reversible spontaneous polarization. In the recent years this switchability of polarization has been demonstrated to have applications in non-volatile memories for computer systems. Since then many laboratories all over the world are engaged in solving problems related to applications involving polarization reversal. In this thesis we investigate some aspects of ferroelectric capacitors directly relevant to such applications. Before starting our problem, we introduce the necessary concepts briefly in the following sections.

1.1 Ferroelectric Ceramics

For the study of fundamental properties of the ferrolectric materials initially single crystal samples were used because they provide the advantage of having less imperfections

and surface effects. Ferroelectric ceramics, on the other hand have the advantage of being a great deal easier to prepare than their single crystal counterparts. In many cases, they show ferroelectric properties approaching quite closely to those of the single crystals. In addition, it is possible to prepare wide range of ceramic compositions and to tailor the characteristics of the material properties for different applications.

1.2 Lead Zirconate Titanate (PZT)

Of the many known ferroelectric ceramics lead zirconate titanate (PZT), a solid solution obtained from lead zirconate and lead titanate, has attracted considerable attention of the researcher because of its potential applications as pyroelectric detectors, piezoelectric transducers and in opto-electronics devices. The PZT ceramics are chemically represented by $Pb(Zr_xTi_{1-x})O_3$. They are perovskite solid solutions of antiferroelectric $PbZrO_3$ and ferroelectric $PbTiO_3$, and can exist in any of three crystal structures: tetragonal, rhombohedral and orthorhombic. Above a certain temperature called Curie temperature, the ceramic has a cubic structure and is paraelectric. On cooling below the curie temperature, a phase transformation occurs to tetragonal or rhombohedral structure depending upon the composition occurs. To minimize the accompanying stresses, each grain of the ceramics break into domains. In a domain the polarization is directed along the crystallographically allowed directions. The net polarization of a sample is zero due to random orientation of domains. When a sufficiently high electric field is applied, domains tend to align along the field direction and the ceramic attains a net polarization. This process is called poling. In the phase diagram of PZT, a sharp phase boundary between the rhombohedral and the tetragonal phases called the morphotrophic phase boundary (MPB) exists at the composition of $Pb(Zr_{0.53}Ti_{0.47})O_3$. The compositions in the MPB region are of immense technological importance because of high values of piezoelectric coefficients, large remnant polarization and reasonable coercive field etc. The samples used in this work have compositions near the MPB.

1.3 Advantages of Thin Film over Bulk Ceramics

Bulk materials, both single crystals and ceramics still dominate research activities in ferroelectric materials. However, thin ferroelectric film research activities have recently taken large strides. Several phenomena in ferroelectric materials such as polarization hysteresis, pyroelectricity and electro-optic activity are exploited to make integrated devices on semiconductor IC chips. The advantages of thin films over bulk counterpart are

- Crystallization and sintering temperatures of thin films are usually hundreds of degree centigrade lower than for bulk counterpart and also compatible to semiconductor processing temperature.
- Due to submicron thickness, operating voltage is usually few volts (corresponding to high field) only which is compatible to electronic circuit drive voltage.
- High charge storage density in small area leads to miniaturization of devices.
- Epitaxial growth is relatively easier in thin film form than to single crystals of a bulk counterpart.

1.4 Ferroelectric Thin Films

The first report of ferroelectric thin film growth involved the materials of perovskite structure. In 1955 Feldman [1] reported the synthesis of micrometer thick $BaTiO_3$ on Pt by flash evaporation. These films were amorphous as-deposited and had to be heated to above 1100^{0}C to obtain polycrystalline films with a low dielectric constant. Later Moll [2] and Muller et al from Philco Scientific Labs., used a grain by grain evaporation technique to attempt a epitaxial growth. Muller et al [3] reported the first successful vapour phase growth of epitaxial films of wide variety of simple perovskites on LiF heated to about 600^{0}C. In the beginning of 1970 synthesis was dominated by the newly developed rf sputtering technique. The capabilities of obtaining desired properties in thin film significantly widens the scope of applications. Rapid progress has been made in thin film devices in the last decade mainly due to developments in various growth techniques.

1.5 Preparation Techniques of Ferroelectric Thin Films

In general, film deposition techniques can be divided into dry and wet processes. Dry processes include sputtering, evaporation, whereas the common wet processes are Metallo-Organics Deposition (MOD) and sol-gel. The wet processes usually use unheated substrate or low temperature deposition, whereas dry processes use a range of temperatures, typically unheated substrates to 700^0C. As an example, MOCVD is done at elevated temperature due to the necessity of hot substrates. With exception of MOCVD, all other dry processes involve physical vapour deposition (PVD). The major PVD technique differ among themselves in several ways, particularly in the energetics of flux incident on the substrate during film growth. Techniques such as, rf-sputtering and ion beam sputtering tend to have large amounts of energetic species incident on the growing film due to large target voltages, whereas evaporation usually involves very small energy flux at the substrate. Laser deposition and magnetron sputtering involve intermediate level of energetic bombardment of the substrate. All these techniques have been successfully used to prepare PZT thin films. However, among these techniques sol-gel route is probably the best as regards formation of perovskite phase, homogeneity of composition and control over thickness. In this work we use exclusively sol-gel route to prepare films. Sample preparation details are given in Chapter 2.

1.6 Motivation of this Work

In this section we provide only a broad motivation behind this work, leaving the precise definition of the problem to a later section. One recent application of ferroelectric thin films is their usage in non-volatile computer memories based on their bistable polarization state which can be switched from one state to another by applying an external voltage. Attempts were made in 1950's and 60's by several researchers in this direction. But at that time one

of the major obstacles was the lack of proper deposition technique that could achieve high quality sub-micron ferroelectric thin films. Earlier ferroelectric memories [4] employed bulk material that resulted in switching threshold of the order of tens or hundreds of volts and the switching speeds in the range of microseconds to milliseconds, rendering the technology incompatible with the silicon IC technology.

However, with the advent of modern thin film deposition techniques to produce sub-micron ferroelectric thin films, it has been possible to reduce operating voltages to levels compatible with microelectronics. Ferroelectric thin films are currently being studied for both nonvolatile random access memory (NVRAM) [5] as well as dynamic random access memory (DRAM) applications. But the commercial viability of these memories is dictated not only by the cost but also by their long-term time performance. There are several phenomena which degrade the properties of a ferroelectric capacitor used as a memory cell. Among them, fatigue is the degradation of the sample polarization by repeated switching and it has been studied by many authors in some detail [6]. The phenomena of depolarization is related to the short time retention properties [7]. The current lack of detailed understanding of mechanisms leading to degradation phenomena is perceived as a major stumbling block. There has been little progress in tuning processing conditions to improve these properties. Specially, there has been controversy as regards the origin of depolarization as a phenomenon itself. The primary motivation behind this work is to correlate effect of annealing ambient during preparation of sol-gel derived PZT films with electrical properties. We first provide a brief review of effect of ambient during annealing, and recent depolarization study as a background to the statement of the present problem.

1.7 Effect of Annealing Ambient: A Brief Review

There have been some limited recent reports on the influence of annealing ambient on the properties of thin films. Chikarmane et al [8] had done a detailed study on the effects of post-deposition annealing on the properties of sputtered PZT thin films. They deposited

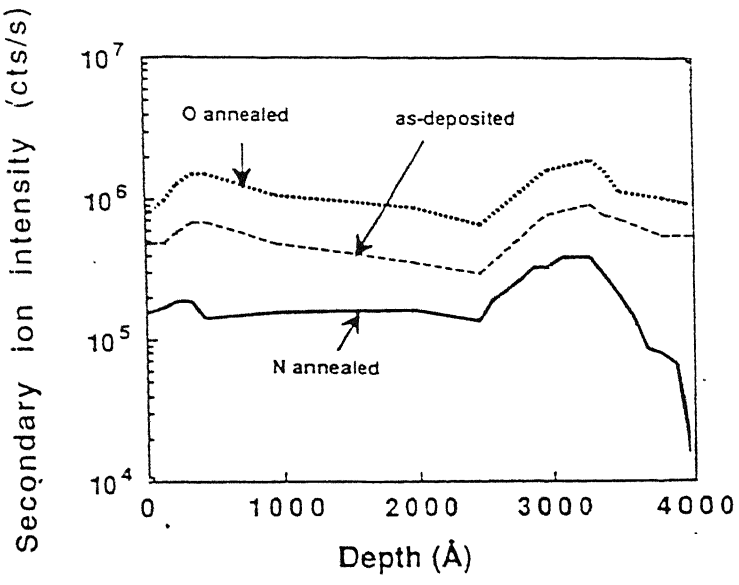

Fig. 1.1 SIMS depth profile of oxygen content for as-deposited sputtered PZT thin films, and films annealed in O_2 and N_2 ambient (Ref: Chikarmane et al [8])

PZT films of morphotropic composition having thickness 4000 A^0 on $Pt/TiO_2/SiO_2/Si$ substrate using reactive magnetron sputtering. The wafer was then scribed into chips (38×7.5mm) for use in annealing experiments. The films were furnace annealed either in an O_2 or N_2 ambient at temperature ranging from 625 to 700 ^{0}C. Top electrode are deposited over the films by lift-off methods.

To find out the concentration of oxygen across the thickness of the film they did the compositional depth profile study using secondary ion mass spectroscopy (SIMS). The SIMS depth profile of oxygen content as obtained by them is given in Fig. 1.1 . From the figure it is clear that films annealed in N_2 show a large depletion in oxygen content in the bulk while an increase in oxygen content is shown by films annealed in O_2. They conclude that nitrogen annealed films have more oxygen vacancies than the oxygen annealed films.

When I-V measurement were done in these films, they found that the N_2 annealed films had low degradation field and dielectric breakdown voltage than those annealed in oxygen ambient. Such low values in N_2 annealed films were attributed to the higher concentration of oxygen vacancies in nitrogen annealed films. Similarly it was also observed that due to

larger concentration of mobile oxygen vacancies, the fatigue rate in N_2 annealed films is faster than O_2 annealed films.

There has been no similar study on sol-gel derived films. On the basis of studies in our laboratory Majumder et al [9] have recently reported that nitrogen ambient helps perovskite phase formation . Improvement in ferroelectric parameters was also noted.

1.8 Depolarization Studies: A Brief Review

To the best of our knowledge, very few works devoted exclusively to depolarization phenomena in PZT thin films have been published. Benedetto et al [10] studied the effects of operating conditions on the fast decay components of the retained polarization in PZT films. They simulated the write (read) conditions that would be experienced by the ferroelectric film in a nonvolatile memory circuit. Based on their experiments, Benedetto et al proposed a model to explain the fast decay components of polarization. According to their model time dependent depolarization fields cause partial reversal of polarization. Benedetto et al explain their model as follows: To some extent depolarization fields always exist in thin insulating ferroelectric thin films due to extent of finite separation between the polarization charge and the compensating free charges in the electrode[11]. If the polarization is essentially constant upto the immediate vicinity of the electrodes then depolarization fields are generally small. However, if a gradient in the polarization exists over some appreciable distance near the electrode interfaces or the compensating charges in the electrodes is distributed over a finite screening distance or especially if there are non-switching layers in the ferroelectric film near the interfaces then the depolarization field may be significant. Indeed since the depolarization fields are in a direction opposite to that of the bulk polarization, partial reversal of polarization may occur if the magnitude of depolarization field exceeds the coercive field. In turn, the depolarizing fields relax as the reverse switching occurs with the process ceasing when depolarizing field drops approximately to the value of coercive field.

Benedetto et al obtained only the quantitative loss of polarization with different time delays between the read and write pulses, but the exact nature of decay of polarization in this time interval was not studied.

Mihara et al [12] carried out an extensive study of depolarization behaviour in sol-gel derived PZT by utilizing four consecutive pulses instead of conventional positive and negative double pulses. They propose a model for depolarization by attributing the origin of depolarization field to the standard capacitor connected to the sample in depolarization measurements. This field is called external depolarizing field. When the input voltage goes to zero, the top plate of the standard capacitor would still be at higher potential and hence produce a depolarizing field. But, the depolarization phenomenon has been reported in resistor loaded circuit also. In this case Mihara et al explain the depolarization on the basis of an interfacial capacitor in the sample and this interfacial capacitor is similar to that of model proposed by Benedetto et al.

Recently Ramesh [13] had adopted a new measurement sequence to study the depolarization behaviour of sol-gel derived PZT thin film. They carried out P-E measurements alongwith explicit observation of depolarization characteristics in the time domain. The sequence they adopted is as follows: They first take the sample to a desired polarization state through the application of a external voltage, the sequence of which is same as that of one normally used in P-E measurements. Then, a square voltage pulse is applied to force the sample to either change it's existing polarization state or to augment the existing state and then the remnant polarization is monitored as a function of time in the absence of external voltage. They measure hysteresis loops before and after measurements to detect possible changes in other electrical parameters such as internal bias E_i, coercive field E_c etc. They also measured the depolarization characteristics with respect to pulse height, pulse width and temperature. Their results can be summarized as follows:

The hysteresis loop exhibited asymmetry along the field axis indicating the presence of internal bias E_i which favours a definite polarization state in the sample. The internal bias can be changed by applying an external voltage pulse. They show that there exists a define relationship between achieved polarization state and the final orientation of internal bias E_i.

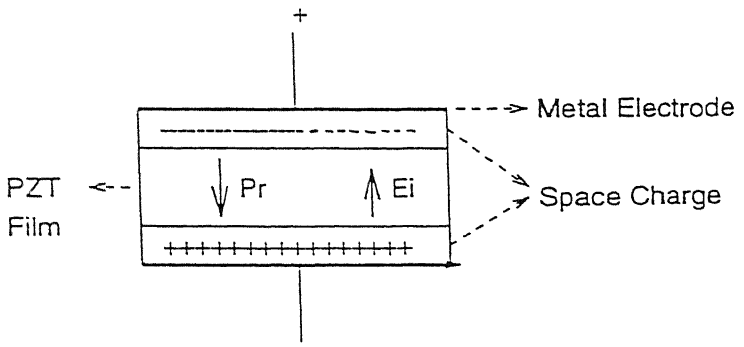

Fig. 1.2 Schematic Showing Origin of Depolarizing Field (Ref: Ramesh [13])

In their measurement they not only observed loss of polarization but also backswitching of polarization state.

They used an isothermal technique called time analyzed transient spectroscopy to analyze the polarization decay curves. They found that decay of polarization to be exponential. From the exponential nature of decay of polarization they conclude that the value of opposing depolarizing field remains constant in the absence of external voltage.

Their measurement with respect to pulse height, width and temperature show that depolarization behaviour is independent of these parameters.

To explain the observed phenomena, Ramesh propose a new model based on the depolarizing field arising from the asymmetry of charge distribution in the interfacial space charge regions, due to trapping (detrapping) of charge carriers while applying an external voltage pulse. Their proposed model invokes existence of defect complexes. Details of their model is given below.

As the depolarizing field developed in response to the applied field is in the direction opposite to the net polarization, and remains constant in the absence of the external field, the origin of the depolarizing field and internal bias lies in the space charge layers at the interface. The net charge developed in the space charge region on application of applied field is such that the field developed is opposite to the external field. For example, in a particular case, the space charge configuration may be as shown the Fig. 1.2. The charge

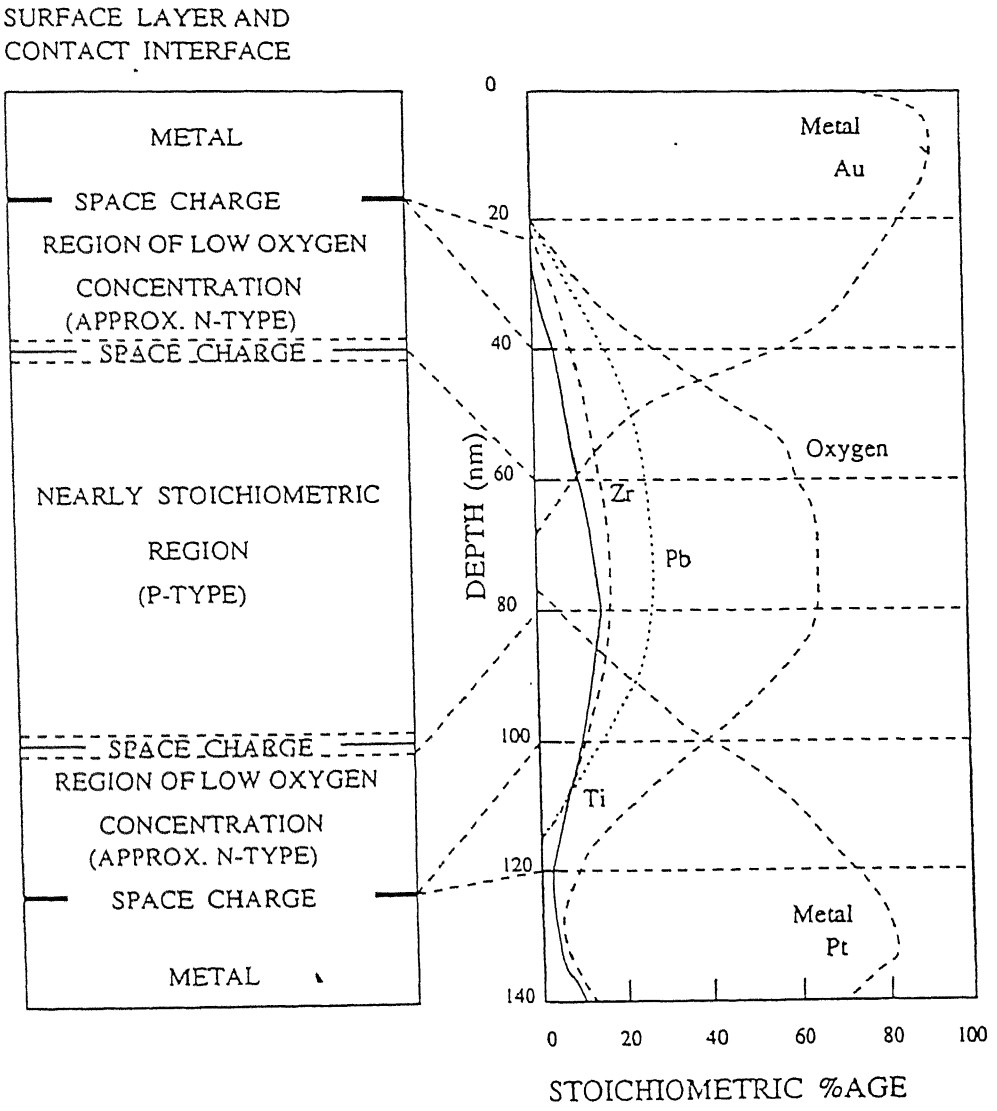

Fig. 1.3 Auger Microprobe Data for PZT Film with PT and Au Electrode

(Ref: Scott et al [14])

developed must be immobile so that the field due to domain polarization is unable to make them move. This points to the involvement of immobile species such as lead vacancies. On the basis of these clues they develop a scenario concerning the origin of the space charge.

Scott et al [14] studied the effects of space charge regions on the electrical characteristics of the PZT thin films prepared by sol-gel technique. They carried out Auger measurements to find out the variation of oxygen vacancy concentration normal to the film. The results of the measurements are reported in Fig. 1.3. It can be noted that the oxygen concentration is not same throughout the film: Rather it decreases sharply near the metal electrodes. It drops to approximately 50% of it's value in the center of the film, while still 20nm from the Pt surface. This creates a oxygen deficient region that may be n-type in contrast to p-type PZT throughout the interior of the film. The oxygen deficient region is present near both the electrodes. Ramesh argue that trapping and detrapping effects of defect associates in this region control depolarization and internal bias.

Clearly the origin of depolarization and internal bias remains controversial.

1.9 Definition of the Problem

From the review it is clear that there has been very little systematic study of ambient on the properties of PZT thin films. Preliminary work on phase formation in nitrogen annealing ambient in our laboratory raised sufficient hopes that ambient of annealing can be used as a processing parameter in optimizing film properties. In this work, we evaluate the effect of annealing ambient on electrical properties of sol-gel derived thin films such as dc leakage current, ferroelectric hysteresis loop, fatigue resistance and depolarization in absence of external electric field. Since there has been no systematic reports on how these phenomena are controlled by processing conditions, such a study is likely to give valuable clues regarding their origin and simultaneously pave the way for their effective control.

Thin PZT films are prepared using sol-gel route. Two distinct heat treatment schedules are used keeping nitrogen as the ambient during annealing. The films are characterized

using XRD, ferroelectric hysteresis loop measurements, current-voltage characteristics and depolarization studies. The results of the measurements are correlated with different combination of ambient and heat treatment schedule. The results corresponding to these measurements for oxygen annealing ambient are taken from earlier studies for comparison. An annealing ambient different from oxygen is likely to clarify the role of oxygen vacancies and other related defects in determining the properties of thin films.

The organization of this thesis is as follows. Chapter 2 has the details of sample preparation and description of experimental set-up. Chapter 3 contains the details of measurements, results and the discussion of results. Chapter 4 is a brief summary of conclusions drawn and scope for future work in this field of research.

Chapter 2

Experimental Details

2.1 Introduction

A wide variety of preparation techniques have been employed to produce PZT thin films such as sputtering, sol-gel, chemical vapour deposition (CVD) , electron beam evaporation and laser ablation [15, 16, 17, 18]. The choice of an appropriate preparation technique depends on the final application of these ferroelectric films. The requirements for use in the electronic application such as memories, are very stringent, and some of the major requirements are strict control of stoichiometry, uniform deposition over a large area (diameter around 100mm to 200mm), high deposition rate and high throughput. Among the techniques mentioned above, sol-gel process offers the advantages of molecular homogeneity, high deposition rate, high throughput and excellent composition control. In addition, the deposition can be under ambient conditions and it is easy to introduce dopants into the films. All the samples for the present work were prepared utilising the sol-gel method.

2.2 Sol-Gel Method

Sol-gel technology provide a method of fabrication of high quality ceramics and glasses. The term sol represents the solution of sub-micron particles and gel represents the interconnected porous mass obtained from the sol. In the recent years, this technique has been extended to fabrication of thin films or coatings on different substrates. In particular, it has been used extensively in production of films of materials such as ferroelectric PZT, high

temperature super-conductor yttrium-barium copper oxide, conducting coating such as indium tin oxide, and optical and protective coatings of complex oxides [19].

There are essentially two different kinds of sol technology. The first, a colloidal method, involves dispersion of colloidal particles in a liquid to form a sol, and then destabilization of the sol to produce a gel. The second method involves the polymerization of organo-metallic compounds, such as alkoxides, to produce a gel with a continuous network [20]. In the present work, the PZT thin films were prepared using the second method.

In the present context, the term sol-gel is used to describe chemical processes in which the polymeric gels are formed from metallo-organic starting solutions. The most commonly studied sol-gel systems are based on the chemistry of the metal alkoxides $M(OR)_n$. Many of these species readily undergo hydrolysis and condensation reactions , leading to oligomer formation and eventual gelation. The key steps in the gel forming reactions can be summarized as follows:

HYDROLYSIS

$$-\overset{|}{\underset{|}{M}}-OR + H_2O \rightarrow -\overset{|}{\underset{|}{M}}-OH + R-OH$$

CONDENSATION

$$-\overset{|}{\underset{|}{M}}-OH + R-O\overset{|}{\underset{|}{M}}- \rightarrow -\overset{|}{\underset{|}{M}}-O-\overset{|}{\underset{|}{M}}- + R-OH$$

$$-\overset{|}{\underset{|}{M}}-OH + HO-\overset{|}{\underset{|}{M}}- \rightarrow -\overset{|}{\underset{|}{M}}-O-\overset{|}{\underset{|}{M}}- + H_2O$$

For thin film work, the gel forming solutions are coated onto suitable substrates by spin-on, dip or spray coating techniques, after which drying and firing stages convert the gel coating to oxide film. In the present study, PZT thin films were prepared by spin coating technique.

In sol-gel processing, chemicals for preparing films are dissolved in a liquid to form a solution. Since all the starting materials are mixed at the molecular level in the solution a high degree of homogeneity of film can be expected. Another advantage of the sol-gel process is that because of the solution form of raw materials, trace elements can be easily introduced into the solution by adding the element in the form of organo-metallic compounds or soluble organic/inorganic salts. Such trace elements can be used in adjusting the microstructure or in improving the properties of the oxide films [21].

2.3 Preparation of $Pb(Zr_{0.53}Ti_{0.47})O_3$ Thin Films

PZT ceramics are chemically represented by $Pb(Zr_xTi_{1-x})O_3$. They are perovskite solid solutions and can exist in any one of the three crystal structures: tetragonal, rhombohedral and orthorhombic. The boundary between tetragonal and rhombohedral phases at x = 0.535 is a sharp morphotopic phase boundary (MPB). The compositions in the MPB region are of great technological interest because of high values of piezoelectric coefficients, large remnant polarization, reasonable coercive field etc. Hence for the present work samples with morphotrophic composition (x = 0.535) have been prepared.

Precursor solution for the preparation of films are prepared utilising modified sol-gel processes proposed by Desu [18]. The starting materials for the preparation of the sol are lead acetate, zirconium-n-propoxide, titanium-4-butoxide and acetic acid. The acetic acid is used as a chelating agent to increase the shelf life of the precursor solution. To prepare the film a small amount of stock solution was taken and calculated amount of propanol and acetic acid were added to it. The relative amounts of various chemicals used in a typical sol are given in Table 2.1

A 5 mole% of excess lead was used to compensate for any lead loss during the heat treatment cycle.

Platinum substrates have been used in this work as it is convenient for electrical contact. Also it is known that high quality PZT films are obtained on it. Prior to film

deposition, platinum substrates are polished mechanically using velvet cloth and 1μm Al_2O_3 particles

Table 2.1

Chemicals used in Preparing the Sol

S.No.	CHEMICALS	MOLES
1	Lead acetate	1.05
2	Acetic acid	6.60
3	Zirconium-n-propoxide	0.53
4	Titanium-4-butoxide	0.47

dispersed in water. The polishing is continued till a mirror finish is obtained. The polishing is necessary to remove any pinholes and surface imperfections which may lead to poor quality films. The substrates were then cleaned using the cleaning procedure as shown in Fig. 2.1. This cleaning procedure is aimed at removal of thin layer of oxide and impurities on the surface.

2.3.1 Spin Coating

The substrates are coated with the sol using spin coating technique. The platinum substrate is fixed on the head of a Centrifuge (REMI INSTRUMENTS) and rotated at 5000 rpm. A drop of the precursor solution is applied to the substrate using a syringe and the substrate is kept at 5000 rpm for 5 sec. to get a uniform thickness. The uniformity of film thickness is inferred from observation of interference colours of the films. The thickness of film obtained in a single coating is mainly controlled by the viscosity of the solution and spin speed. The viscosity of the solution is directly related to the molar concentration of the solution [22]. The film thickness linearly increases in proportion to the increase in molar

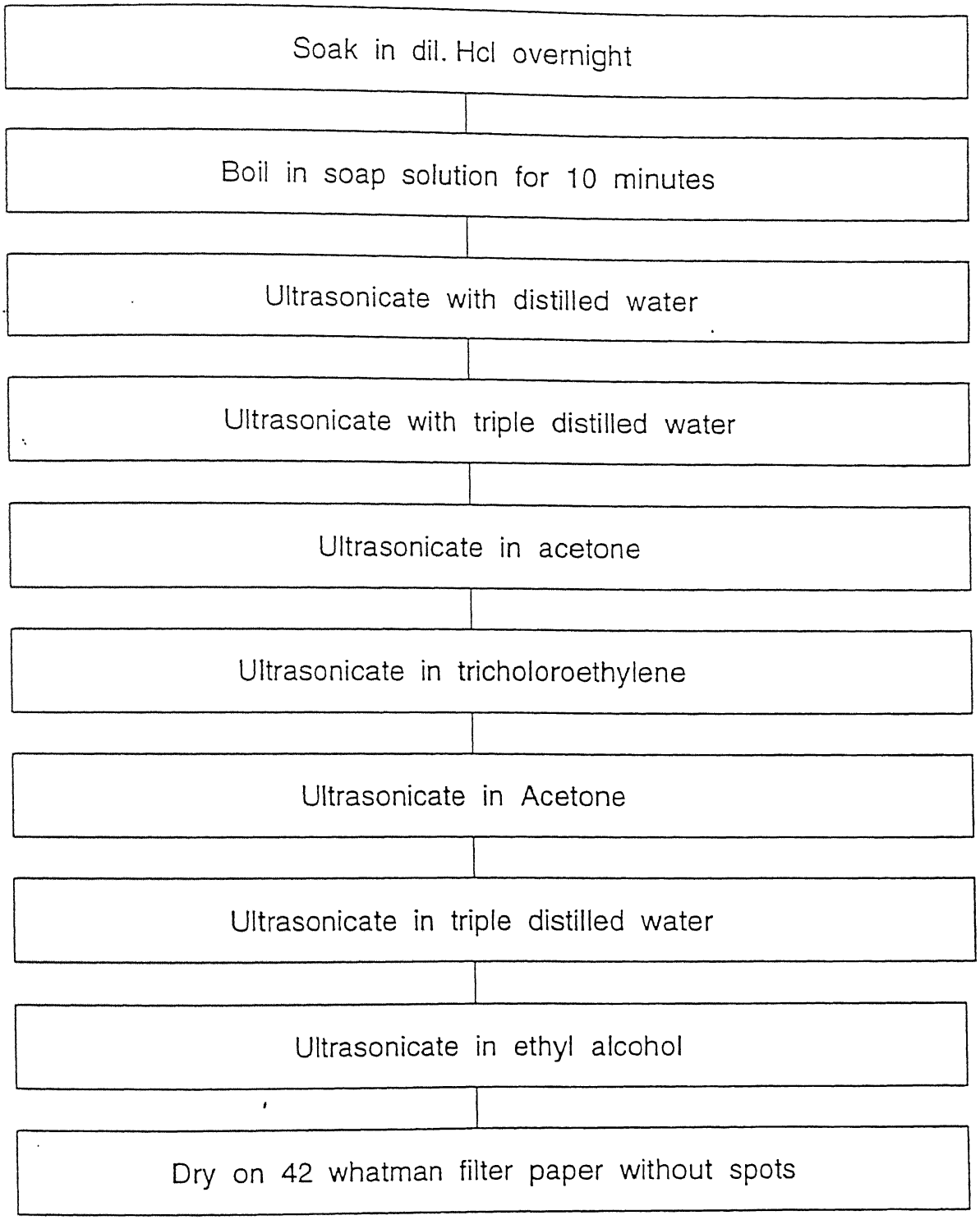

Fig. 2.1 Block Diagram for Substrate cleaning procedure

conc. of the solution. Empirically, film cracking is directly related to the film thickness as well as the heating rate. Film cracking occurs when the thickness in a single coating is larger than a critical value. For PZT films on the platinum substrates, the tendency for the film cracking increases sharply, when the molar conc. of the PZT solution is larger then 0.5M. Therefore the molar conc. of the solution used in this work are kept between 0.25 - 0.3M range.

The film thickness can also be controlled by the spin speed. The relationship is given by the equation [18]

$$t = kw^n$$

where, t = film thickness,

k = constant depends on evaporation rate, viscosity, diffusivity and molecular weight of the solvent,

n = - 0.5

w = spin speed in rpm

2.3.2 Firing and Annealing

Two types of firing and annealing as proposed by Majumdar et al [23] were used in this work. After each coating the film was fired at 400^0 C in air for 15min. to drive out the organics present in the film and then quenched to the room temp. The film thickness can be increased by repeating the spin coating-firing sequence. After required thickness is obtained, the film was inserted at 700^0C in nitrogen ambient for final annealing. The typical annealing time is one hour. For some samples, we used annealing duration of 6hours. The films obtained by such a heat treatment are referred to as low intermediate rapid fired (LIRF) sample.

In the second case, after each coating the film was fired at 600^0C for 15 min. in air do drive of the organics. The spin coating-firing sequence was repeated to obtain the desired film thickness. After this film was suddenly inserted into the furnace at 700^0C in nitrogen

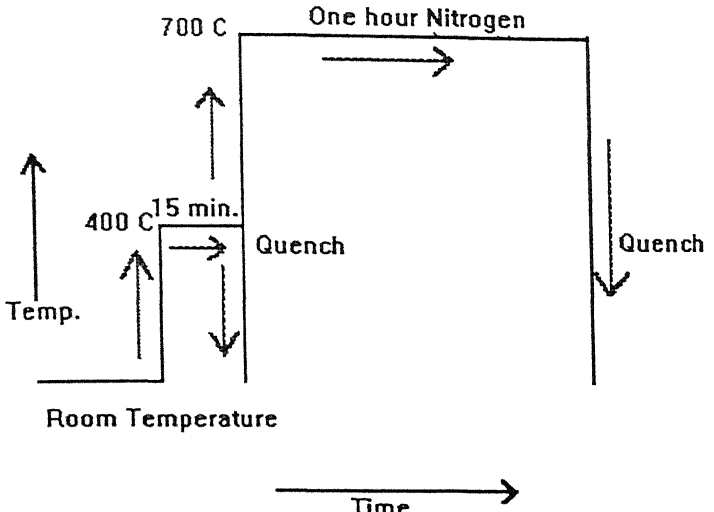

Fig. 2.2 Heat treatment for LIRF Sample

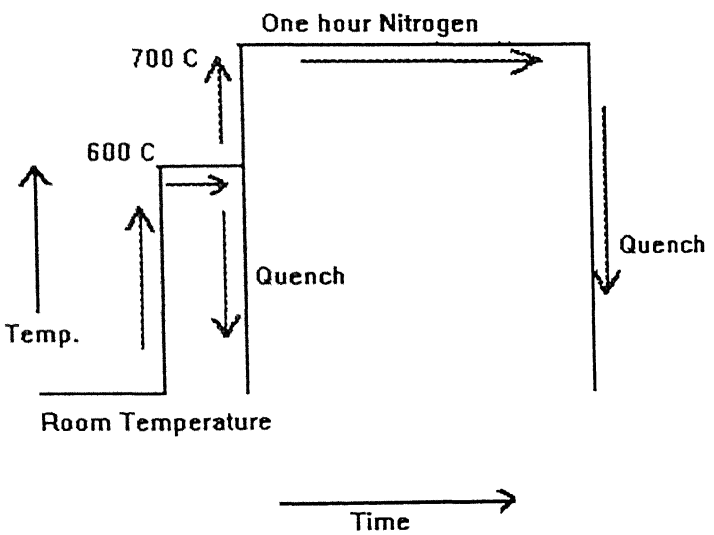

Fig. 2.3 Heat treatment for HIRF Sample

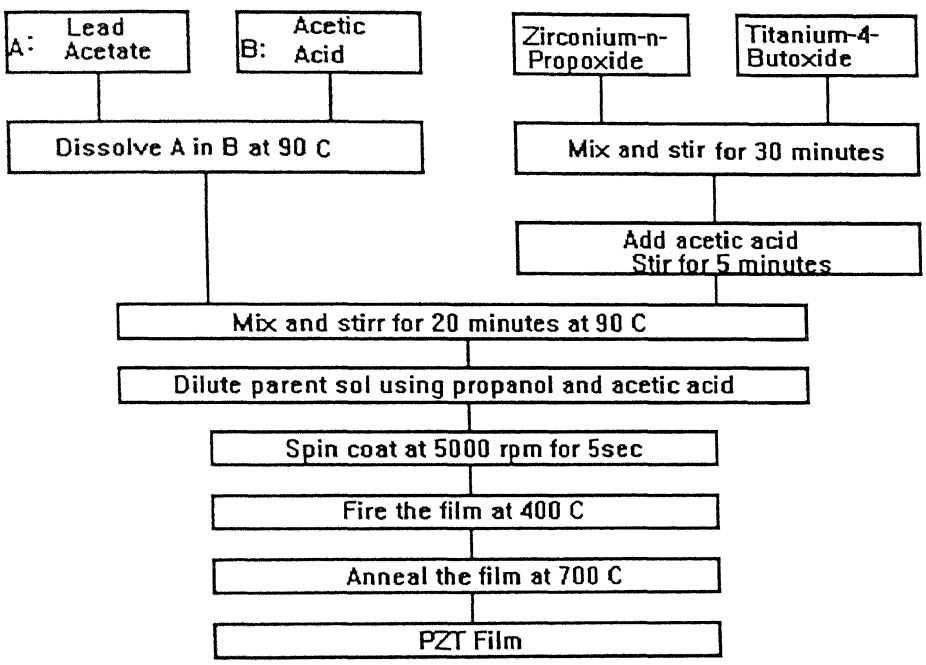

Fig. 2.4 Flow diagram for preparation of PZT thin films

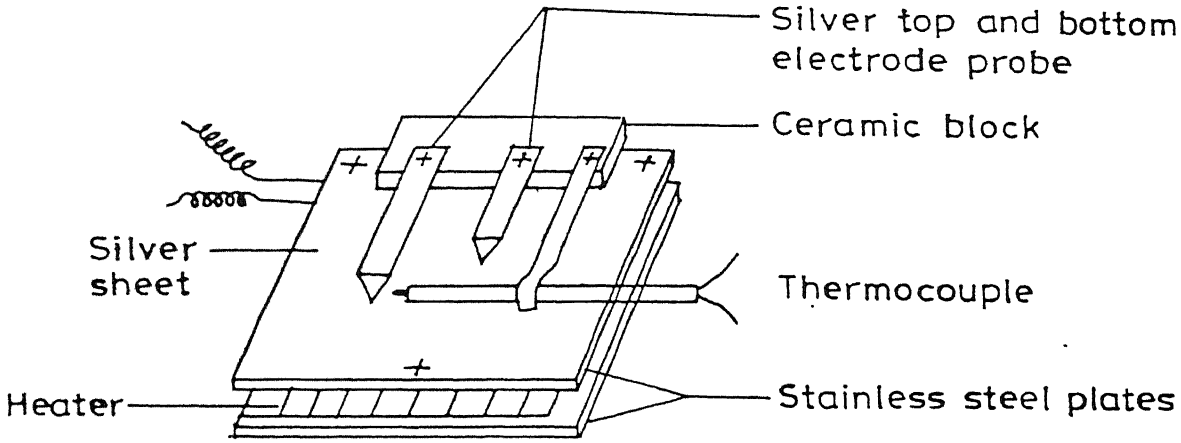

Fig. 2.5 Sample Holder for P-E Measurements

ambient and annealed for one hour. The film obtained in this method are termed as high intermediate rapid firing (HIRF). The schematic of the heat treatment adopted for LIRF and HIRF samples are given in Fig. 2.2 and Fig 2.3 respectively.

The flow diagram of the preparation of PZT films using the modified sol-gel process is as given in Fig. 2.4.

2.4 Experimental Details

2.4.1 Description of the Sample Holder

The sample holder used in the hysteresis and depolarization measurement is shown in Fig. 2.5. It has been made using the Ag-Cu alloys. The probes used in it for making electrical contacts to the sample are mounted on the base using a teflon block. The sample holder has an additional arrangement for temperature measurement. For heating the sample to desired temperature, it has been equipped with 16Ω heater coil.

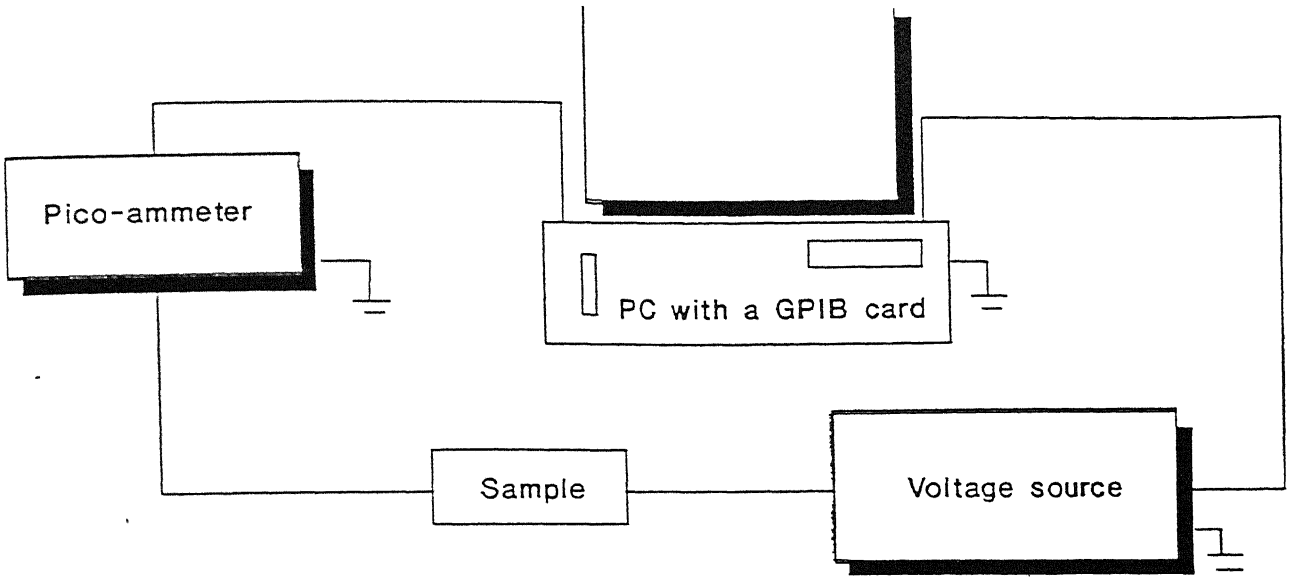

Fig. 2.6 Schematic of setup for I-V Measurements

2.4.2 Experimental setup for I-V measurements

For current voltage measurement we used an automated setup as given in the Fig. 2.6. Here a programmable voltage source (Keithley 230) is used for bias application and auto ranging picoammeter (Keithley 485) is used for measuring currents. These two are interfaced with a personal computer (Zenith PC XT 286) for automatic recording and storage of data. For measurements, voltage are raised from 0 volts to the desired voltage with a step of 1 volts. The time between two successive voltage step is kept at 1sec.

2.4.3 Experimental set-Up for Hysteresis Measurements

The hysteresis measurement are carried out using the conventional Sawyer-Tower circuit [24]. The schematic of Sawyer-Tower circuit and it's implication are given in Fig. 2.7 & 2.8. By measuring the voltage across the standard capacitor, the polarization value of the sample can be determined. A bipolar triangular voltage of desired peak voltage is

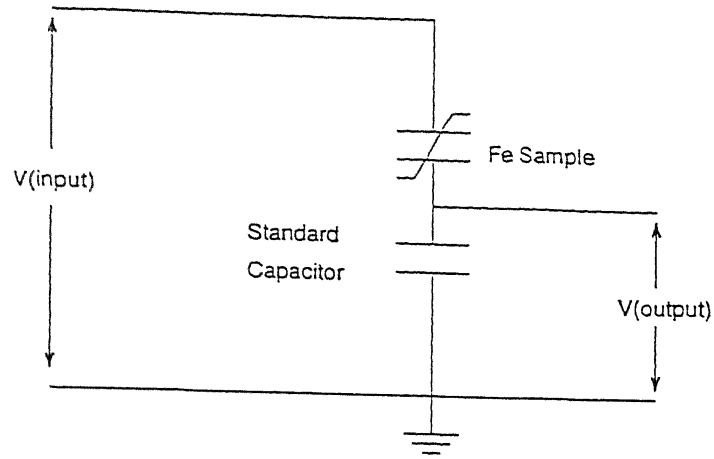

Fig. 2.7 Schematic of modified Sawyer-Tower circuit

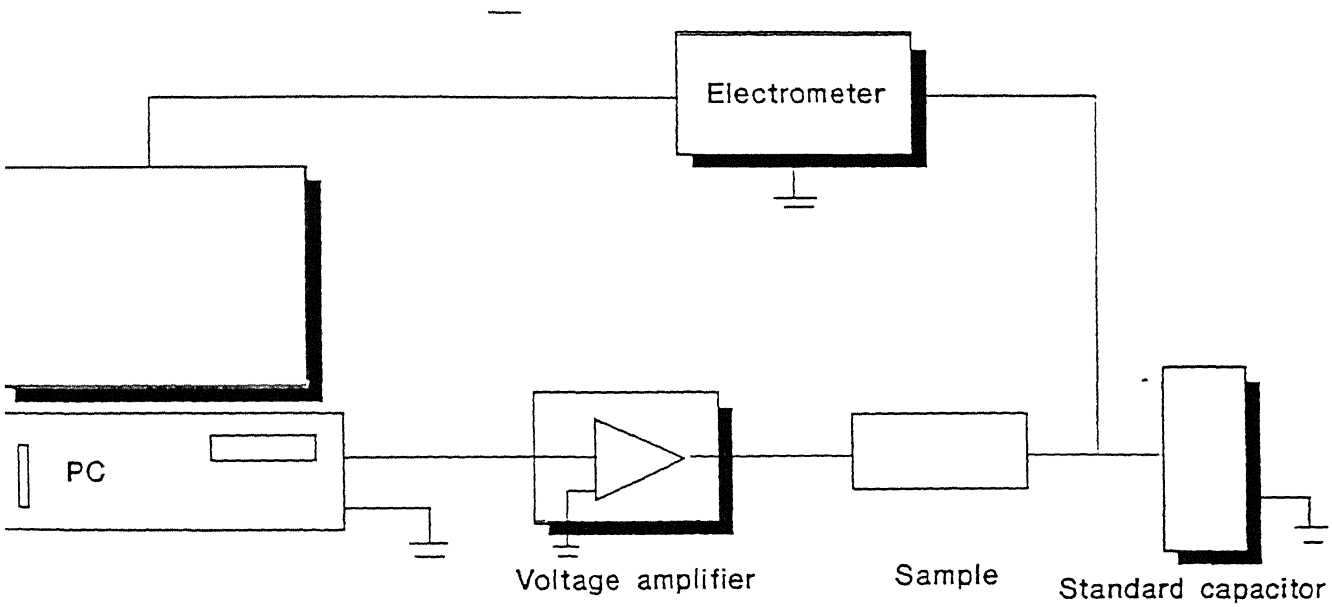

Fig. 2.8 Schematic of implementation of Sawyer-Tower circuit

generated at 0.4Hz using the computer. The voltage is then amplified by the bipolar voltage amplifier (KEPKO BOP10000M). The amplified voltage is then applied across the sample-standard capacitor combination. The standard capacitance is usually very large compared to the sample capacitance so that most of the applied voltage drops across the sample.

The voltage across the standard capacitor is measured using the electrometer (KEITHLEY 610C) which has very high input impedance ($10^{14}\Omega$). The value of the standard capacitor used in our work is 225nF. The output of the electrometer is read back using the AD card and the reading are stored in a data file. The sample polarization is calculated according to the following equation

$$P = Q/A$$

or $$P = C\, V_{out}/A$$

where, P = sample polarization, C = capacitance of the standard capacitor, V_{out} = voltage across the standard capacitor, and A = area of the sample capacitor.

2.4.4 Description of Set-up for Depolarization Measurements

The depolarization measurements were also carried out using the conventional Sawyer-Tower circuit. A square voltage pulse of desired magnitude is generated using an D/A add-on card in the computer. The voltage pulse after amplification using the bipolar voltage amplifier (KEPKO BOP1000M) is applied across the sample-standard capacitor combination. By measuring the voltage across the standard capacitor, the polarization of the sample is calculated. The polarization is monitored as a function of time. To enable recording of long transients, the sampling time interval between the data points is chosen to be different for each decade of time.

Chapter 3

Measurements and Results

3.1 Sample Details

The $Pb_{1.05}(Zr_{0.53}\ Ti_{0.47})O_3$ thin films used in this work are prepared by sol-gel method. To study the effect of ambient during the final stage of annealing, two different heat treatment sequences are used. In all the samples N_2 ambient is used in the final stage of sintering.

In the entire work the following nomenclature is used to name different samples.

Low Intermediate temperature Rapid Fired (LIRF) Sample:

During repeated coating of films to obtain the desired thickness, the film is fired at 400 ^{0}C in air for 15min after each coating. After obtaining the desired thickness, the film is annealed at 700 ^{0}C in N_2 ambient. Those samples which are annealed for 1hr are called LIRF(1hr N_2) and those for 6hr are called LIRF(6hr N_2).

High Intermediate temperature Rapid Fired (HIRF) Sample:

During repeated coating step, the film is fired at a higher temp of 600 ^{0}C in air for 15min. After obtaining the desired thickness the film is annealed at 700 ^{0}C in N_2 ambient for 1 hour. These samples are called HIRF(1hr N_2).

Similar notation has been adopted while referring to oxygen annealed samples obtained by other workers in our laboratory.

For measuring hysteresis loops and depolarization characteristics of the samples, circular Au-Pd electrodes of diameter 0.5mm are deposited on both LIRF and HIRF

samples. The electrodes are deposited using the sputtering unit (Hummer VA-Anatech Ltd.) operating at 80 mtorr in argon ambient.

3.2 Thickness measurements and X-ray Pattern

The thickness of the films used in this work is measured using Double Beam Spectrometer (Hitachi 150-20) in reflectance mode. The method depends on spectral dependence of interference of light reflected from a thin film. Spectrometer was scanned for a range of wavelength starting from 200 nm to 900nm to obtain a set of fringe patterns. From the wavelengths corresponding to these maxima and minima of fringe patterns, the film thickness are calculated using the formula given below.

If d′ is the thickness of the film then,

$$d' = \frac{\lambda_1 \lambda_2}{2[n(\lambda_1)\lambda_2 - n(\lambda_2)\lambda_1]} \qquad \text{.....3.1}$$

where λ_1 and λ_2 are the wavelengths corresponding to two adjacent maxima or minima.

and $n(\lambda_1)$ and $n(\lambda_2)$ are the refractive indices of the film at two wavelengths λ_1 and λ_2 respectively.

For each adjacent maxima and minima d′ was calculated and from that average d′ , $\overline{d'}$ was calculated. This value of $\overline{d'}$ was put in the standard interference fringe formula to get m′

$$2\, n\, \overline{d'} = m' \lambda \qquad \text{.....3.2}$$

samples. The electrodes are deposited using the sputtering unit (Hummer VA-Anatech Ltd.) operating at 80 mtorr in argon ambient.

3.2 Thickness measurements and X-ray Pattern

The thickness of the films used in this work is measured using Double Beam Spectrometer (Hitachi 150-20) in reflectance mode. The method depends on spectral dependence of interference of light reflected from a thin film. Spectrometer was scanned for a range of wavelength starting from 200 nm to 900nm to obtain a set of fringe patterns. From the wavelengths corresponding to these maxima and minima of fringe patterns, the film thickness are calculated using the formula given below.

If d′ is the thickness of the film then,

$$d' = \frac{\lambda_1 \lambda_2}{2[n(\lambda_1)\lambda_2 - n(\lambda_2)\lambda_1]} \qquad \text{.....3.1}$$

where λ_1 and λ_2 are the wavelengths corresponding to two adjacent maxima or minima.

and $n(\lambda_1)$ and $n(\lambda_2)$ are the refractive indices of the film at two wavelengths λ_1 and λ_2 respectively.

For each adjacent maxima and minima d′ was calculated and from that average d′ , $\overline{d'}$ was calculated. This value of $\overline{d'}$ was put in the standard interference fringe formula to get m′

$$2\, n\, \overline{d'} = m' \lambda \qquad \text{.....3.2}$$

m′ is rounded to nearest integer for maxima and half integer for minima to get true m.

Putting this value of m in eq. 3.2, true thickness d is calculated and from that average d is obtained which is the thickness of the film.

Fig. 3.1 and Fig. 3.2 show the fringe patterns as obtained in HIRF and LIRF samples. Well defined fringe patterns in both LIRF and HIRF sample confirm the uniformity of the film thickness. The film thickness of HIRF and LIRF sample are determined to be 1.78μm and 1.7μm respectively.

The effect of ambient on phase formation has been studied using x-ray diffractrometer (Richseifern Iso debyeflex-2002 with Cu-Kα radiation and a monochromator). Fig. 3.3. shows the XRD-pattern of LIRF(N_2) and LIRF(O_2) samples. In both the LIRF(1hr N_2) and LIRF (6hr N_2) samples a sharp peak centered around $2\theta = 31^0$ is observed. This is the 100% peak for the tetragonal phase of PZT. Hence this confirms the perovskite phase formation in PZT. Other peaks corresponding to perovskite phase are also present. The peak observed at around $2\theta = 46.5^0$ is due to the platinum substrate.

Perovskite phase was obtained for all the samples studied. However, the 110 peaks in the spectra for LIRF (N_2) are broader than those for LIRF (O_2). This indicates that perovskite phase formation is slower in nitrogen ambient than oxygen ambient keeping all the processing parameter constant. Again the 100 peaks of LIRF (6hr N_2) are sharper than LIRF (1hr N_2) samples. So with increase in annealing time, broad peaks become progressively sharper. As far as X-ray results are concerned, the results are similar for HIRF samples in both N_2 and O_2 ambient.

3.3 Current-Voltage measurement

The leakage current as a function of applied voltage was studied using an automated circuit. The current at different voltage was noted in both LIRF and HIRF sample. For comparison with oxygen ambient the data obtained in our laboratory by Majumder [9]

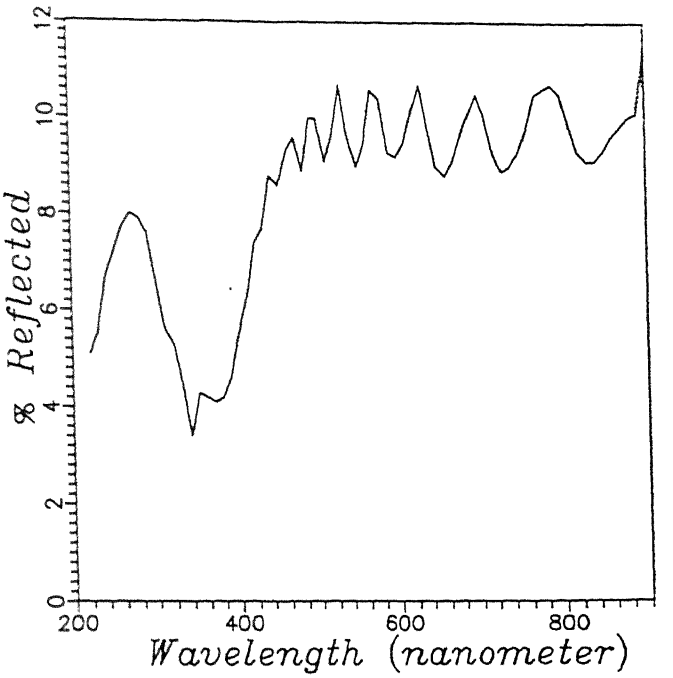

Fig. 3.1 Reflectance Spectra of HIRF Nitrogen annealed sample.

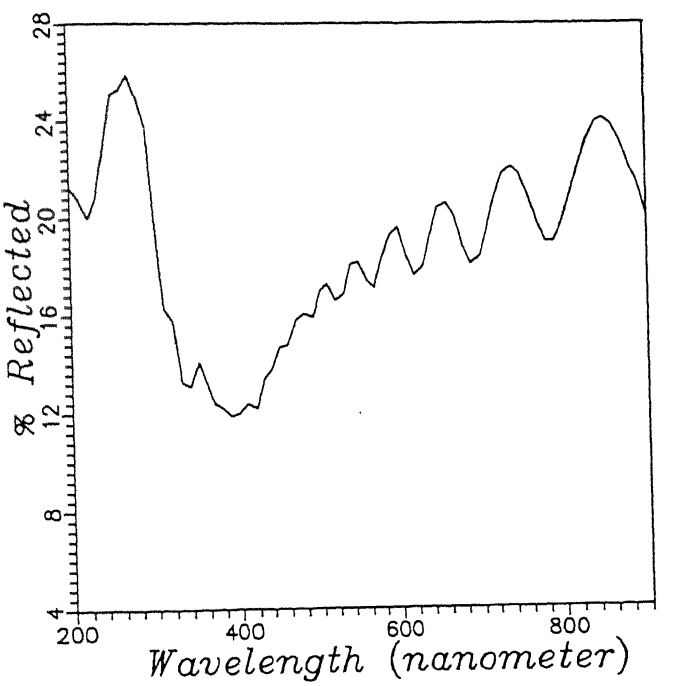

Fig. 3.2 Reflectance Spectra of LIRF Nitrogen annealed sample.

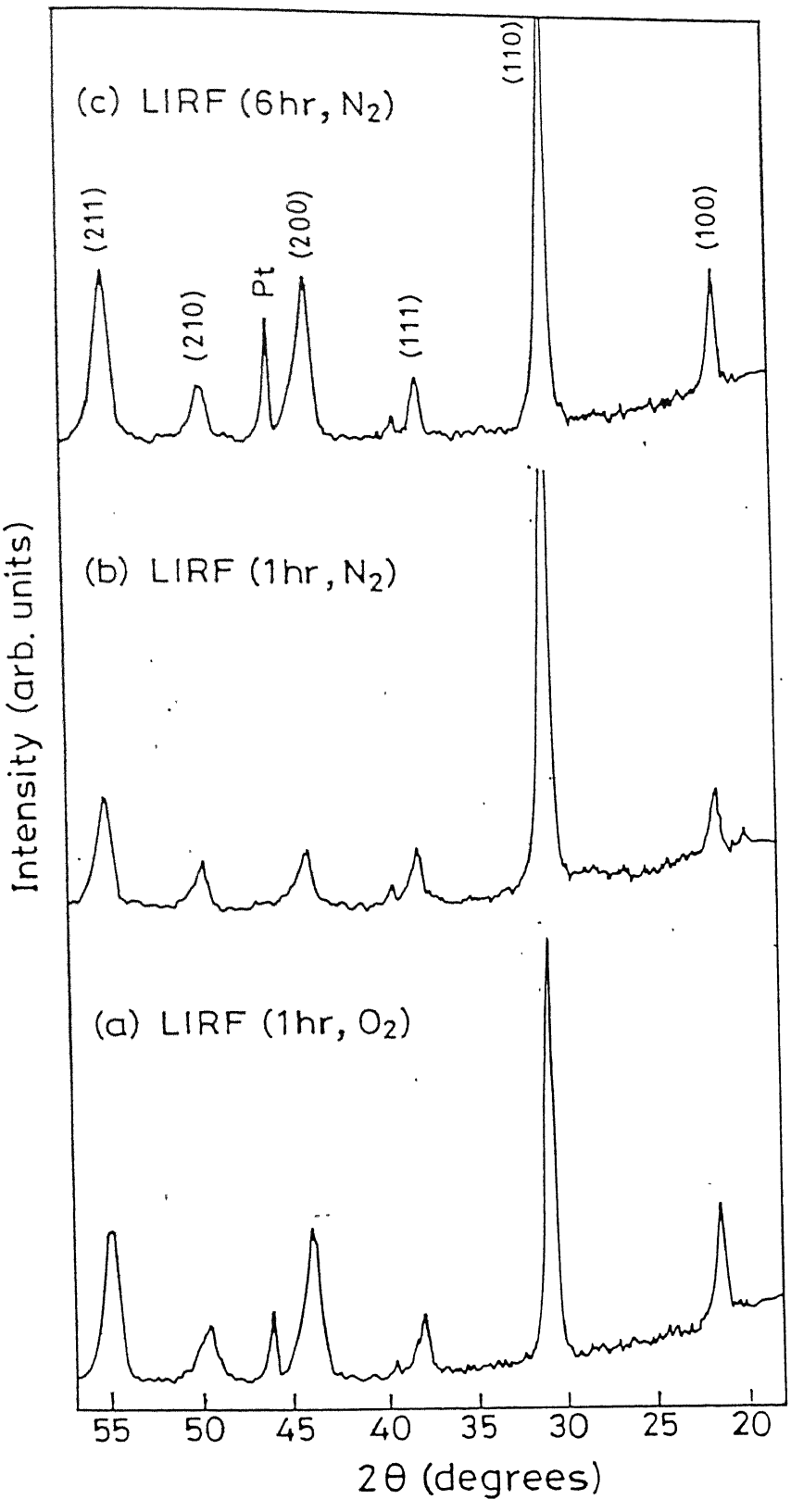

Fig. 3.3 X-Ray diffraction pattern of LIRF (N_2) and LIRF (O_2) samples

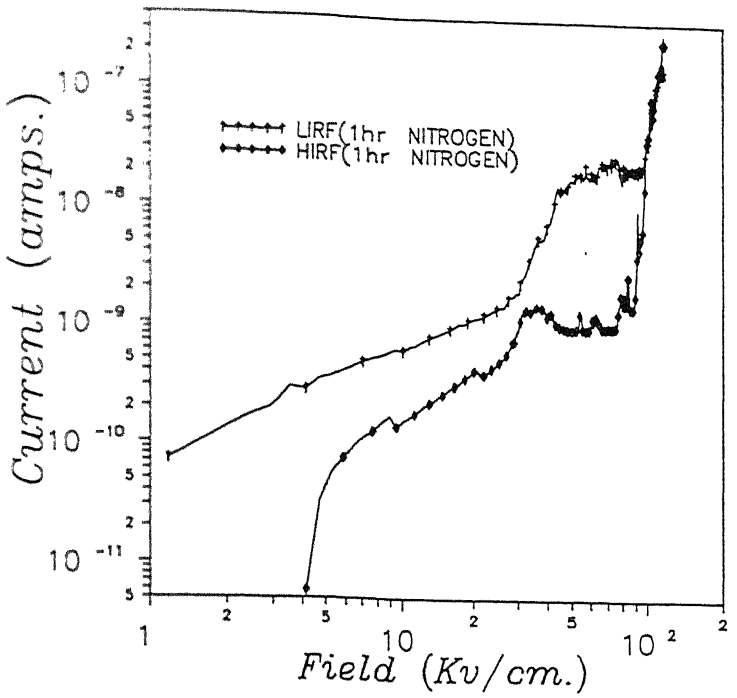

Fig. 3.4 Current–Voltage characteristic of LIRF and HIRF Nitrogen annealed sample

under otherwise identical processing conditions are considered. Fig. 3.4 shows a log(I) Vs log(V) plot of both LIRF(1hr N_2) and HIRF(1hr N_2). Clearly the leakage current is lower in case of high intermediate firing temperature. For HIRF(1hr N_2) sample, the currents are extremely low for low fields. The behaviour indicates that there is a contact potential at the contacts giving rise to diode like behaviour in this low field regime. The peak like structure seen at around the critical field E_c is attributed to current due to switching polarization. At high fields the current shoots up several order of magnitude. This behaviour is common to most sample reported in the literature, though the origin is still controversial. Many authors relate it to onset of trap filled limit culminating finally in a space charge limited current. Others have attributed it to Poole-Frenkel effect and even currents due to injection through the contact [25].

However, as far as comparison between sample from LIRF(1hr N_2) and HIRF(1hr N_2) is concerned, high intermediate temperature rapid firing produces samples with lower leakage current. This observation is opposite to that seen for similarly heat treated samples in

air ambient. Specifically, it is the LIRF samples that had lower leakage current as has been reported by Majumder [9].

Fig. 3.5 shows the log(I) Vs log(V) plot of both HIRF(1hr N_2) and HIRF(1hr O_2). Clearly the leakage current is more in oxygen annealed sample. Log(I) Vs log(V) plot of LIRF(1hr N_2) and LIRF(1hr O_2) are given in Fig. 3.6. Here it is observed that nitrogen ambient produces more leakage current in the sample. This high leakage current in the nitrogen annealed sample is due to presence of a large number of free oxygen vacancies. In oxygen ambient, the oxygen vacancies formed pair and hence the no of free oxygen vacancies is reduced, whereas in nitrogen ambient even if they form pairs, as they are large in number, enough free oxygen vacancies are present to give rise to large carrier concentration.

The degradation of remnant polarization during cycling of the polarization state is referred as fatigue in literature. Here fatigue study is done in both LIRF and HIRF samples. The films were fatigued by applying saturating sinusoidal switching voltages (15-25V) and frequency ranging from 1 KHz to 100 KHz. It is known that oxygen vacancies play an active role in determining the fatigue properties. Larger is the concentration of oxygen vacancies, lesser is the fatigue resistance. Recently Majumder et al [26] have also shown involvement of oxygen vacancies in PZT thin films.

When the films are subjected to 1 KHz cycling, they lost their ferroelectricity. The film either got shorted or the hysteresis loop lost its shape. Even at high frequency of 100 KHz we also observe poor fatigue resistance. This poor resistance to fatigue can be attributed to the presence of large number of oxygen vacancies in the film. In fact our samples provide unambiguous demonstration of the role played by oxygen vacancies in causing fatigue of the samples.

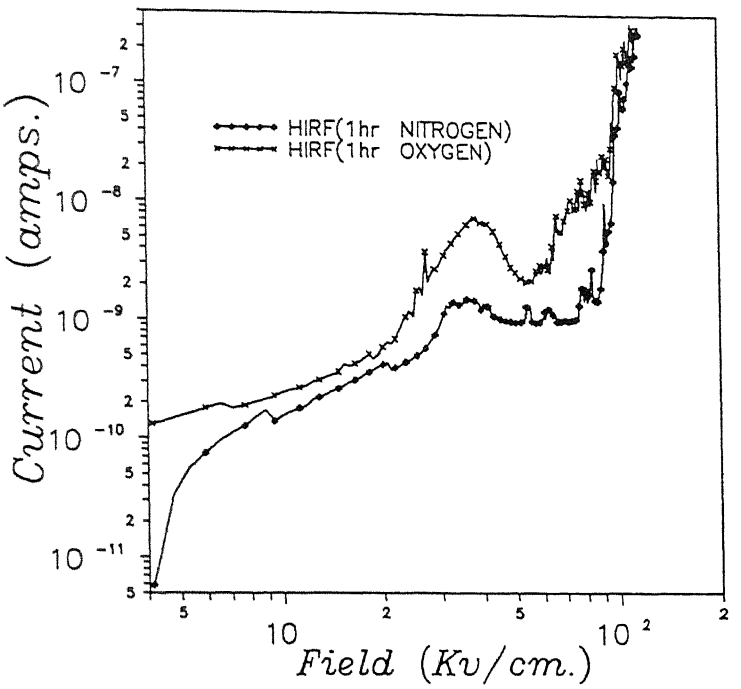

Fig. 3.5 Current–Voltage characteristic of Hirf Nitrogen and Oxygen annealed sample

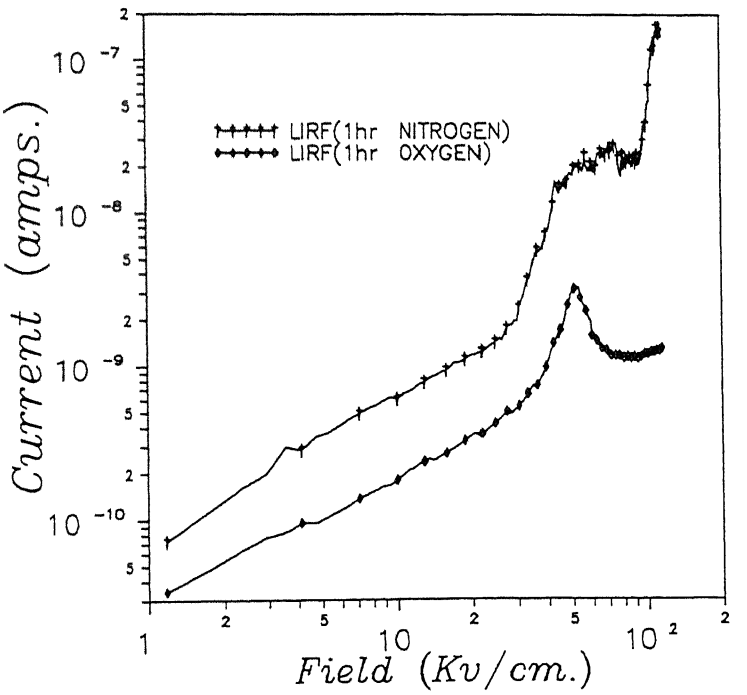

Fig. 3.6 Current–Voltage characteristic of LIRF Nitrogen and Oxygen annealed sample

3.4 Polarization - Electric Field measurement

The polarization of the sample as a function of the applied electric field is studied using an automated modified Sawyer-Tower circuit as has been described in Chapter 2. P-E loop exhibits the expected non-linear dielectric behaviour, i.e., hysteresis which separates ferroelectrics from linear dielectrics. The hysteresis behaviour is because of spontaneous polarization at temperature less than the Curie temperature. At lower field strength in unpolarized material, the polarization is initially reversible and is nearly linear with the applied electric field. At higher field strengths, polarization increases considerably as a result of switching of the ferroelectric domains. At still higher field strengths, the change in polarization is small due to polarization saturation. In this condition, all the domains of like orientation are aligned with the field. Extrapolation of the high field polarization back to zero gives the spontaneous polarization (P_s). When the applied field is increased beyond the value required to achieve P_s, the spontaneous polarization continues to increase but only proportional to initial dielectric constant. When electric field applied to sample is cut off, the polarization doesn't go to zero but remains at a finite value called remnant polarization (P_r). This is due to oriented domains being unable to return to their random state without an additional energy input by an oppositely directed electric field. The strength of the electric field required to make the polarization (P) of the sample to zero is called coercive field (E_c)

In the present study, the P-E measurements are carried out on the freshly prepared sample capacitor. Fig. 3.7 shows the P-E measurement loop of LIRF (1hr N_2) samples. The remnant polarization (P_r) of these samples is 35 $\mu C/cm^2$ and Coercive Field is 32 Kv/cm and whereas Ramesh [13] had reported that with identical processing condition in LIRF (1hr O_2) samples remnant polarization is 35 $\mu C/cm^2$ and coercive field is 64 Kv/cm. So in nitrogen ambient though the P_r remains unchanged E_c falls sharply.

Fig. 3.8 shows the P-E measurement loop of LIRF (6hr N_2) sample. Here one can see that the remnant polarization increase from 35 $\mu C/cm^2$ of LIRF (1hr N_2) sample to

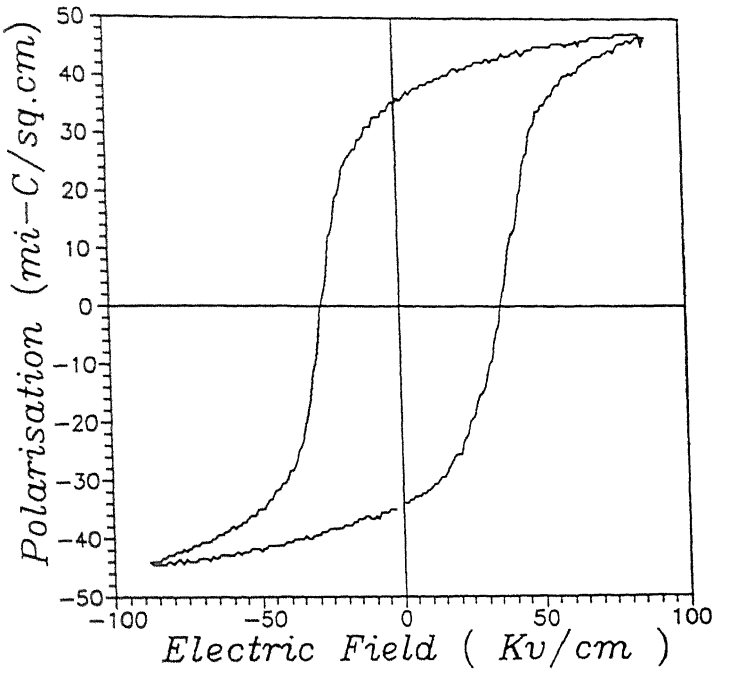

Fig. 3.7 P–E Characteristic of LIRF (1hr Nitrogen) Sample

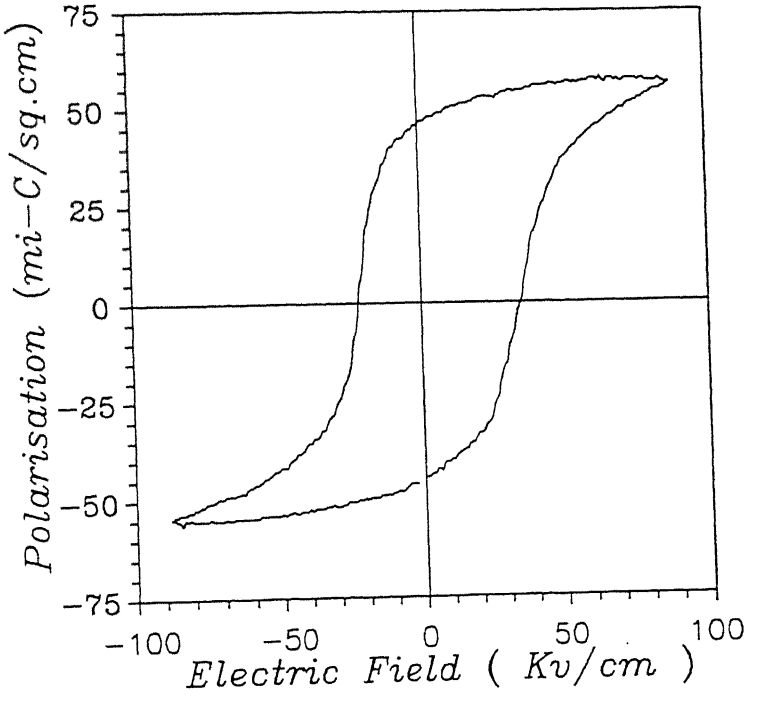

Fig 3.8 P–E Characteristic of LIRF (6hr Nitrogen) Sample

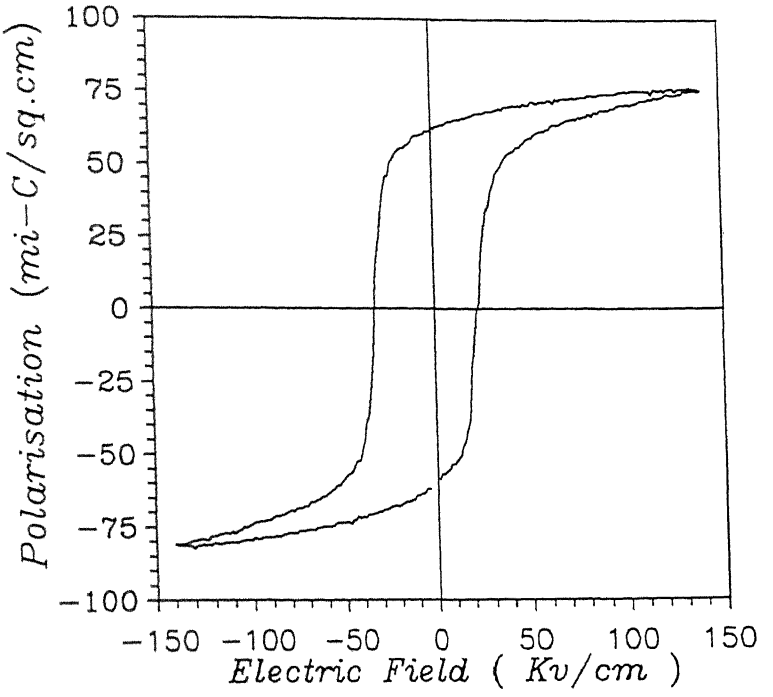

Fig. 3.9 P–E Characteristic of HIRF (1hr Nitrogen) Sample

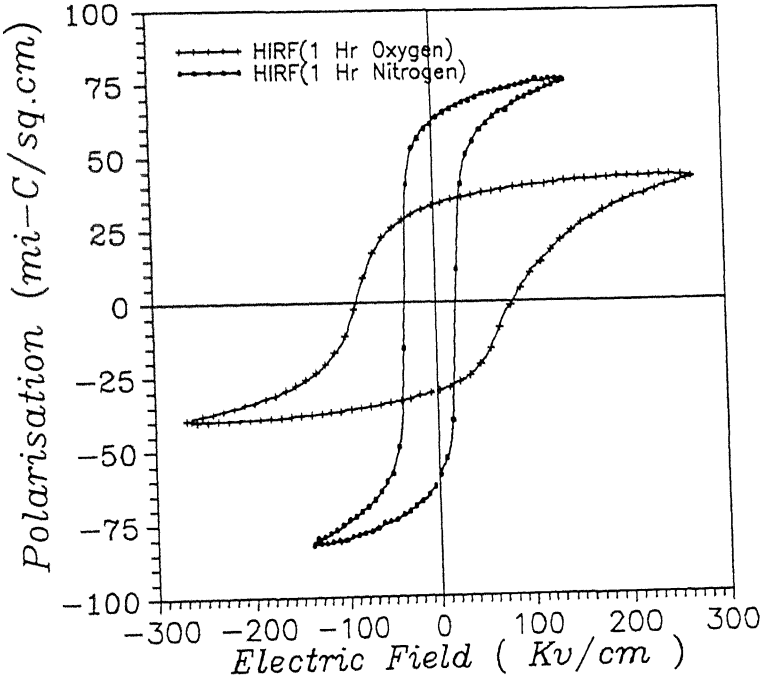

Fig. 3.10 P–E Characteristic of HIRF 1hr Nitrogen and HIRF 1hr Oxygen Samples

45 $\mu C/cm^2$ and coercive field decreases from 32 Kv/cm to 28 Kv/cm. So nitrogen helps in decreasing E_c and increasing P_r of the samples.

Fig. 3.9 shows the typical P-E loop of the HIRF (1hr N_2) samples. Here we get a slim hysteresis loop. The remnant polarization and coercive field of these sample are 60 $\mu C/cm^2$ and 27 Kv/cm. For comparison between nitrogen and oxygen ambient, the P-E loop of HIRF (1hr N_2) and HIRF (1hr O_2) samples are plotted in Fig. 3.10. Here it is clearly visible that in nitrogen ambient the loop becomes slim with low E_c and high P_r values. In oxygen ambient the E_c is 84 Kv/cm where as in nitrogen ambient it is only 27 Kv/cm. In case of P_r in nitrogen ambient annealing it increases from 35 $\mu C/cm^2$ of oxygen to a high of 60 $\mu C/cm^2$. The different P_r and E_c obtained for various processing conditions are given in Table 3.1. For comparison, the P_r and E_c value of O_2 annealed films as reported by Ramesh [13] are also given in Table 3.1 .

Table 3.1

Sample	Pr in $\mu C/cm^2$	E_c in Kv/cm
Lirf (1hr N_2)	35	32
Lirf (6hr N_2)	45	28
Hirf (1hr N_2)	60	27
Lirf (1hr O_2)	35	64
Hirf (1hr O_2)	35	84

It is observed that in contrast to O_2, for N_2 annealed sample the value of P_r is high and E_c is low. In 1hr annealed LIRF sample the P_r value is same for both O_2 and N_2 ambient but E_c of N_2 ambient sample are nearly half of O_2 ambient sample. In 6hr N_2 annealed LIRF sample we get a further increased value of P_r and lesser E_c value in comparison to 1hr LIRF sample. In HIRF 1hr N_2 annealed sample a sharp and distinct change in the value of P_r and E_c are observed. In N_2 ambient the P_r increases from 35 $\mu C/cm^2$ of O_2 to a high of 60

$\mu C/cm^2$ and E_c decreases from 84 Kv/cm to 27 Kv/cm. In some capacitors we get a very high P_r of 84 $\mu C/cm^2$. In all HIRF N_2 annealed sample we get a slim hysteresis loop with high P_r and low E_c.

When P-E measurements are carried out on freshly prepared sample capacitors we observed asymmetry along the field axis. This asymmetry is not a pronounced one. When the P-E measurements are carried for the second time on these fresh capacitors, the hysteresis loops are shifted along the polarization axis but the asymmetry along the field axis is maintained. The shift along the polarization axis (Y-axis) is merely due to the initial potential of the standard capacitor and only need to be subtracted to obtain the true hysteresis loops. However, the asymmetry along field axis (X-axis) has more fundamental physical origin.

Nearly all the P-E measurements carried out in this work, resulted in hysteresis loops exhibiting asymmetry along field axis. Fig. 3.7-3.9 clearly shows the asymmetry along the field axis. In Fig. 3.7 and Fig. 3.8 the coercive field in the +ve field side is more than the coercive field on -ve field side. Whereas in HIRF (1hr N_2) sample the loop is shifted towards the negative field axis sides as shown in Fig. 3.9. An asymmetry is expected along the field axis only when a dc bias is superimposed on the measuring ac field. But, in our measurements there is no such superimposition and it appears as if there is a dc bias naturally existing inside the sample. This bias is called the internal bias and it is calculated from the asymmetry of the hysteresis loops along the field axis as

$$E_i = \frac{E_{c+} - E_{c-}}{2}$$

where, E_i = Field due to internal bias, E_{c+} = Value of coercive filed along the positive field axis, and E_{c-} = value of coercive field along the negative field axis.

Hence the sign of E_i (which determines the orientation of E_i inside the sample) is positive if loop is shifted along the positive field axis and it will be negative, if it is shifted

along the negative field axis. Or in other words, if E_i is positive it indicates that one has to apply higher field to change its polarization state from negative to positive i.e. the negative polarization ($-P_r$) state is more stable Throughout the course of this work, hysteresis loops for many samples under different conditions have been studied. We find a correlation between the asymmetry and sign of saturation polarization exhibited in all these loops. If the field is shifted along the negative field side then the saturation polarization is well pronounced in positive field side. This relation is due to the presence of internal bias inside the sample. The internal bias results are further discussed in relation to depolarization measurements in the next section.

3.5 Depolarization Measurements

3.5.1 Description of the Measurements Sequence

The phenomenon of depolarization is related to short time retention of remnant polarization. Recently a new measurement sequence which monitors the decrease in polarization in the time domain after subjecting the sample to various combinations of polarization sequence was adopted by other workers in our laboratory [13]. Here we also adopt the same procedure. The steps adopted are given below.

1. Polarize the sample to the particular polarization state using P-E measurements. Usually P-E measurements leave the sample in a definite polarization state and hence by changing the voltage sequence applied to the sample during the P-E measurements, the desired polarization state ($+P_r$ or $-P_r$) can be achieved.
2. Polarization of the sample is switched (non-switched) by applying a square voltage pulse. The magnitude of the pulse is equal to the voltage at which polarization of the sample saturates. The width of the voltage pulse can be varied. Once the voltage pulse is applied to the previously polarized sample, the corresponding change in polarization values are monitored as a function of time. The time scale starts when the voltage is

applied to the sample. The typical monitoring time for depolarization measurements is one hour.

3. After the depolarization measurement is over, P-E hysteresis loop is recorded for the sample to monitor any changes in parameters during the course of depolarization.

In step-2, depending upon the polarity of the applied voltage, we will have either switching or non-switching of the previously polarized state. Since the initial polarization state of the sample can be either $+P_r$ or $-P_r$, we will have four different cases, depending upon the initial polarization state and polarity of the applied square voltage pulse. The different combinations are summarized in Table 3.2.

Table 3.2

Initial Polarization state	Polarity of applied voltage pulse*	Final Polarization state	Mention as (S.C : Switching case N.S.C. : Non-switching case)
$+P_r$	Negative	$-P_r$	$+P_r$: S.C.
$+P_r$	Positive	$+P_r$	$+P_r$: N.S.C.
$-P_r$	Positive	$+P_r$	$-P_r$: S.C.
$-P_r$	Negative	$-P_r$	$-P_r$: N.S.C.

* Polarity of the applied voltage is determined w.r.t. top electrode of the sample. If the top electrode is at higher potential than bottom electrode, then the applied voltage is positive and vice versa.

3.5.2 Description of the General Behavior of the Depolarization Characteristics

The depolarization characteristic in general consists of four different regions. The schematic of the four different regions of depolarization characteristics is given in Fig. 3.11.

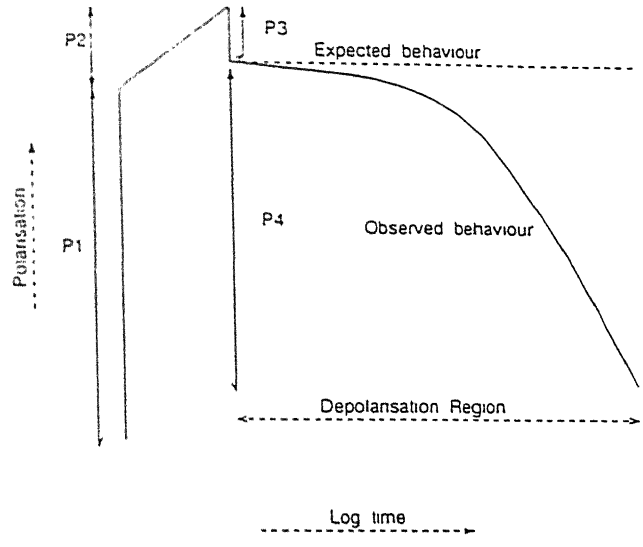

Fig. 3.11 General features of depolarization characteristic of PZT thin film

When a square voltage pulse is applied to the previously polarized sample, there is an instantaneous rise of polarization. The magnitude of rise in the switching cases are large than the non-switching cases. The amount of instantaneous rise of polarization is represented by P1. This instantaneous rise of polarization is due to the fast switching of polarization. In the time interval during which the voltage of the applied pulse remains constants i.e., width of the voltage pulse, there is a comparatively small increase in polarization. The amount of increase of polarization in this second region of depolarization characteristics is represented as P2 . The rise in this region is due to leakage current of the sample, which gets integrated by the standard capacitor used in the depolarization measurements.

When the applied voltage pulse becomes zero, there is an instantaneous loss of polarization. The amount of loss of polarization in this third region of depolarization characteristics is given by P3. The loss of polarization in this region is due to the reverse nucleation of the domains, before applied field value becomes equal to the coercive field.

Ideally, the zero field value of the polarization i.e. remnant polarization should be maintained by the ferroelectric sample for long time. But in the measurements it is observed

that polarization starts to decay from this zero filed value. This fourth region of the depolarization characteristics is called as the depolarization region and amount of loss in this region is given by P4.

In different cases of switching and non-switching of polarization, the loss of polarization is different. In order to get a generalized picture of this loss, the polarization loss at the end of fixed amount of time is given in terms of percentage which is calculated as given below:

Polarization loss = $(P4/P_r)$ X 100%

where P4 = Amount of loss of polarization in the depolarization region, and P_r = Remnant polarization of the sample.

3.5.3 Comparison of Depolarization in LIRF and HIRF Samples

In the present study, the depolarization measurement are carried out on LIRF and HIRF N_2 annealed samples. For all measurements the width of the switching voltage is kept at 5sec. The switching voltage is kept at 15V and 25V for LIRF and HIRF samples respectively. The monitoring time for polarization in the depolarization measurements is one hour. The loss of polarization for all four cases are studied. The value of internal bias before and after depolarization measurements are also noted.

The depolarization behaviour in four different cases of switching and non-switching of polarization of LIRF (1hr N_2) sample are given in Fig. 3.12. The loss of polarization is observed in all four cases. The loss of polarization in $-P_r$: N.S.C. and $+P_r$: N.S.C. is small compared to the switching cases. Fig. 3.13 shows the depolarization behaviour of LIRF (6hr N_2) sample. Here for all four cases of switching and non-switching of polarization the loss is less in comparison to LIRF (1hr N_2) samples. The depolarization behaviour of the HIRF (1hr N_2) sample is given in Fig. 3.14. Here except for the case of $+P_r$: S.C. in all three cases of switching and non-switching of polarization, the polarization loss is small. In

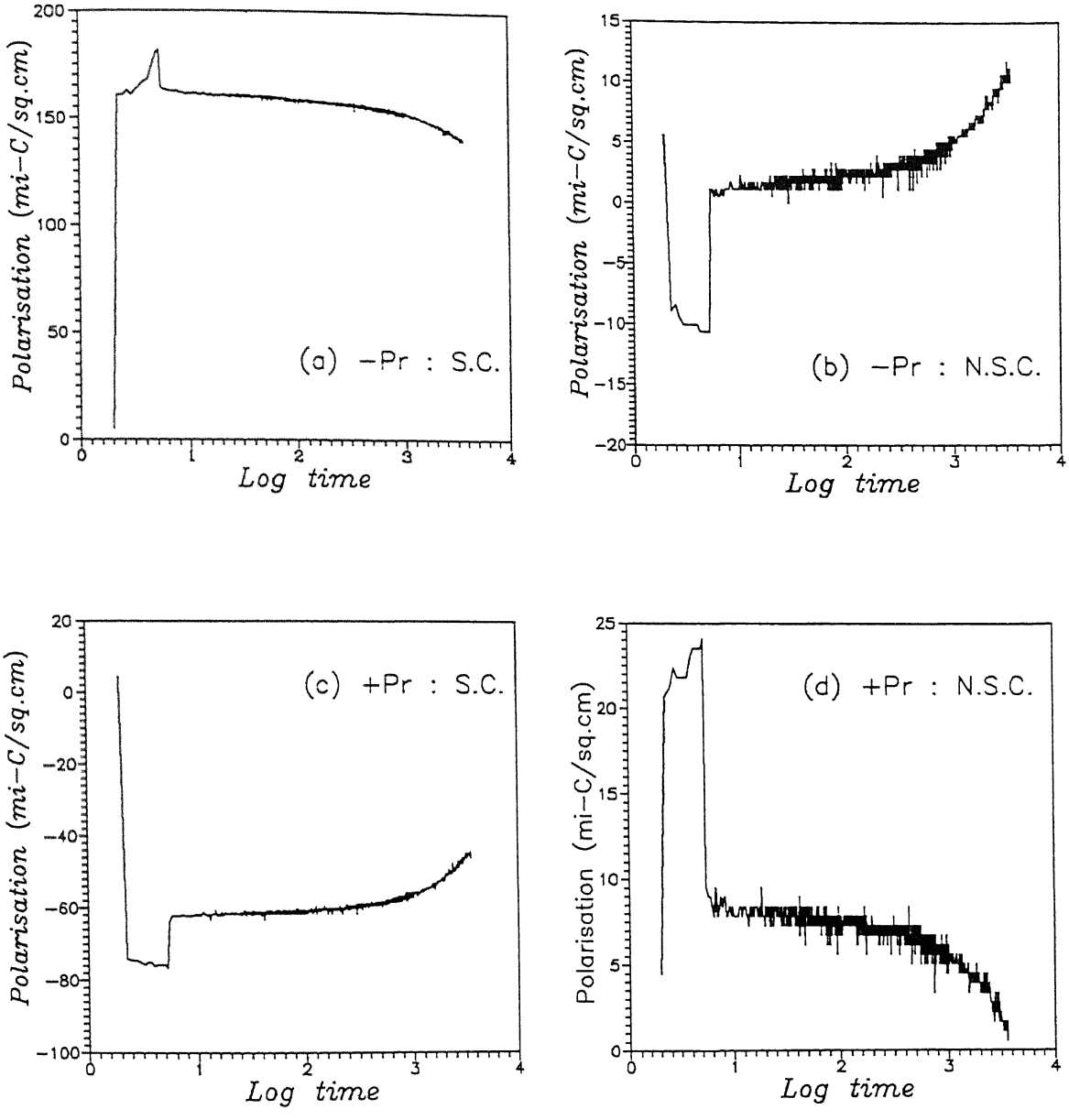

Fig. 3.12 Depolarization behaviour of LIRF (1hr N_2) sample

(a) Initial state $-P_r$: Switched to $+P_r$ (b) Initial state $-P_r$: Non-switched.

(c) Initial state $+P_r$: Switched to $-P_r$ (d) Initial state $+P_r$: Non-switched.

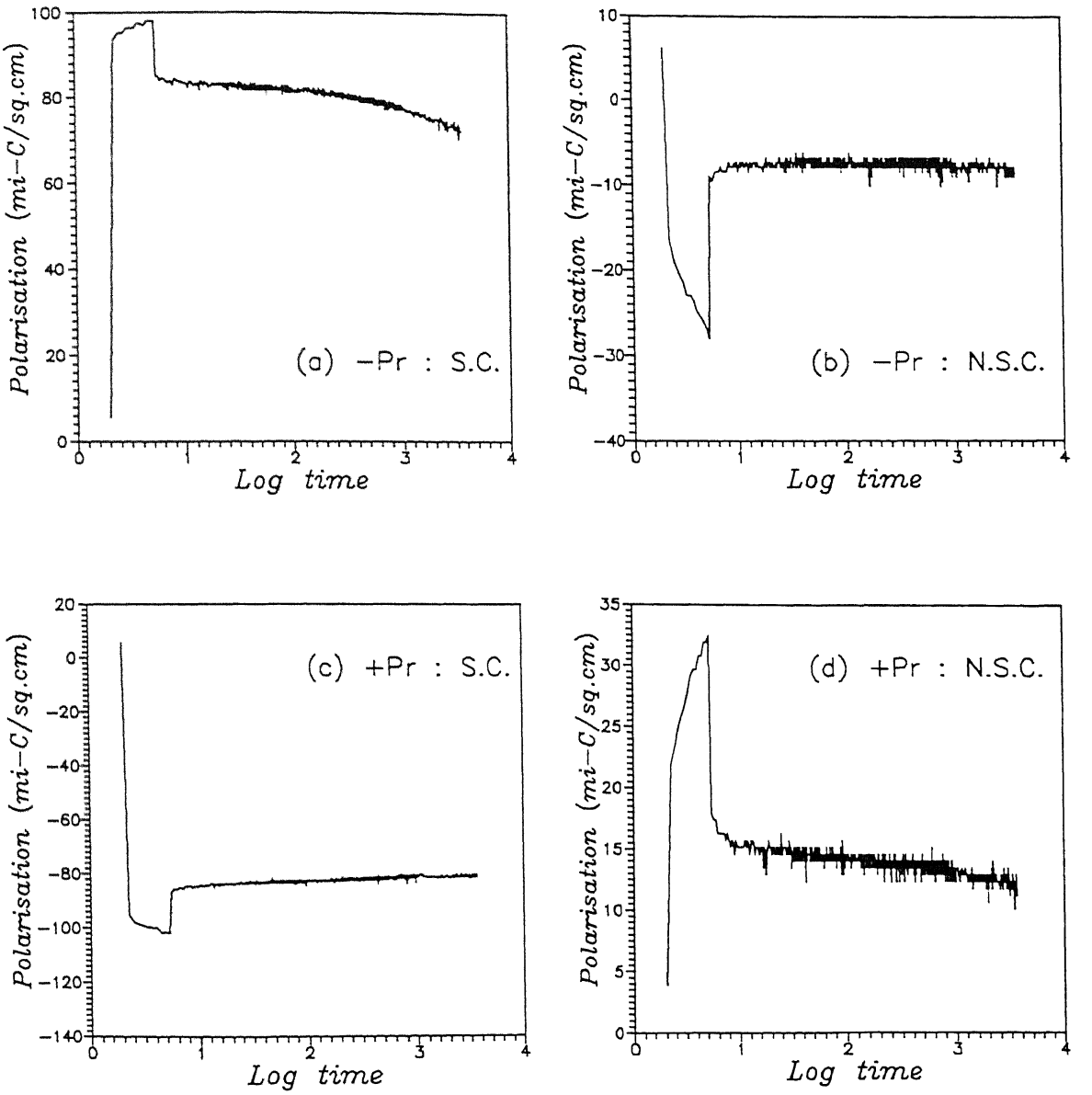

Fig. 3.12 Depolarization behaviour of LIRF (6hr N_2) sample

(a) Initial state $-P_r$: Switched to $+P_r$ (b) Initial state $-P_r$: Non-switched.

(c) Initial state $+P_r$: Switched to $-P_r$ (d) Initial state $+P_r$: Non-switched.

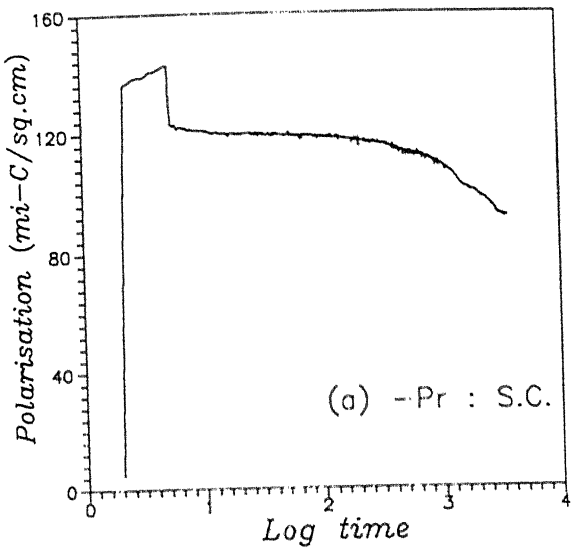

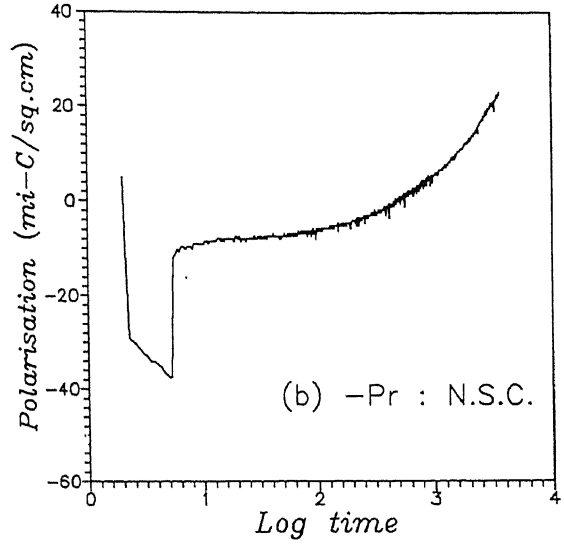

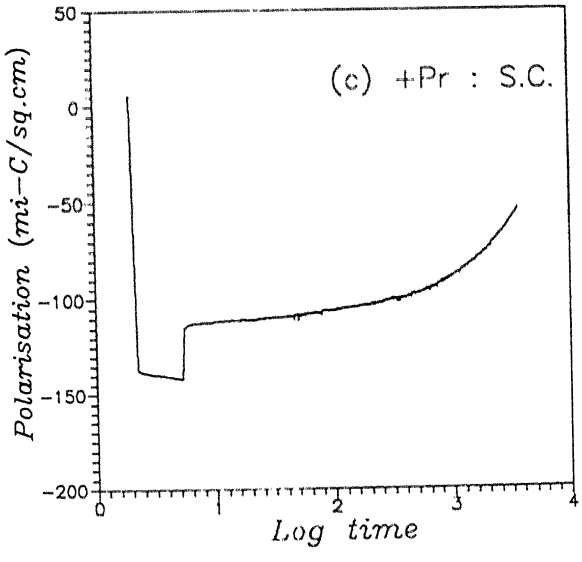

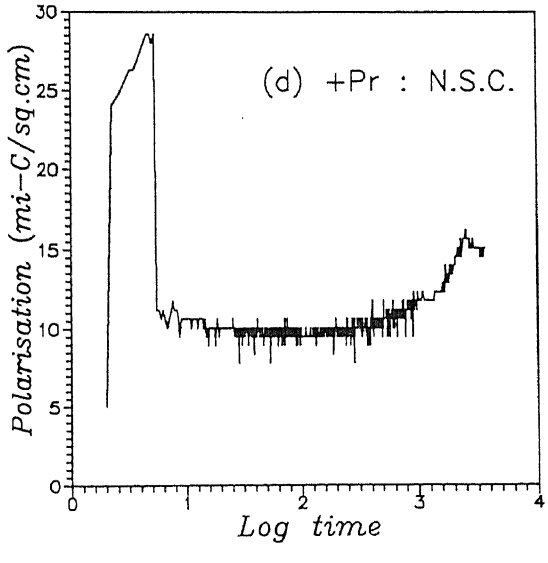

Fig. 3.12 Depolarization behaviour of HIRF (1hr N_2) sample

(a) Initial state $-P_r$: Switched to $+P_r$ (b) Initial state $-P_r$: Non-switched.

(c) Initial state $+P_r$: Switched to $-P_r$ (d) Initial state $+P_r$: Non-switched.

this case the final polarization state after switching and non-switching of polarization try to be in $+P_r$ state and hence the high loss for $+P_r$: S.C. The detailed values of internal bias and % polarization loss for LIRF and HIRF samples along with the values reported by Ramesh [13] are given in Table 3.3 and Table 3.4.

The following inferences can be drawn from the data given.

- The internal bias in the LIRF(N_2) annealed sample are small in comparison to the LIRF(O_2) annealed sample. But in case of HIRF samples the internal bias are nearly same for both N_2 and O_2 ambient.
- In the LIRF samples during the depolarization measurement with four different cases of switching and non-switching of polarization and with respect to all adopted experimental parameters, we observed a strong relation between the polarization state achieved in the depolarization measurements by applying a square voltage pulse, with the orientation of final E_i. If the achieved polarization state is $-P_r$, then the final E_i is found to be positive in sign and if achieved state is $+P_r$, then the final E_i is negative. Similar type of behaviour is reported by Ramesh [13] in both LIRF (O_2) and HIRF (O_2) samples and whereas here in HIRF (1hr N_2) sample this observation sequence is not valid. In HIRF (1hr N_2) sample we observe that for all cases of switching and non-switching of polarization, the final internal bias E_i is always negative.
- In LIRF(N_2) annealed sample the % polarization loss is low in comparison to LIRF(O_2) annealed sample. The study of all the four case of switching and non-switching of polarization are possible in LIRF(N_2) sample, which are earlier not possible in LIRF(O_2) samples. Again between LIRF(1hr N_2) and LIRF(6hr N_2) the % polarization loss in 6 hr N_2 is less.
- In HIRF(N_2) annealed sample we observe that if the final polarization state achieved by applying the square pulse is $+P_r$ then the % polarization loss is very low. But if the final polarization state is $-P_r$ then the % polarization loss is high or comparable with HIRF(O_2) samples. So in HIRF(N_2) sample the $+P_r$ state is more stable then the $-P_r$ state.

Table 3.3

Comparison of % polarisation loss and internal bias values for $-P_r$: S.C. and $-P_r$: N.S.C. in nitrogen and oxygen annealed samples.

	$-P_r$: S.C.			$-P_r$: N.S.C.		
Sample Type	E_i in Kv/cm (Initial)	E_i in Kv/cm (Final)	% Polarization loss	E_i in Kv/cm (Initial)	E_i in Kv/cm (Final)	% Polarization loss
Lirf (N_2 1hr)	3.97	-9.27	72.45	-2.21	0	26.35
Lirf (O_2 1hr)	-	-	-	-10.0	5.0	57.58
Lirf (N_2 6hr)	5.74	-7.06	42.28	-1.33	3.53	1.24
Hirf (N_2 1hr)	-9.83	-16.85	53.14	-9.13	-4.92	58.83
Hirf (O_2 1hr)	-15.0	-21.18	61.05	-21.18	7.5	21.0

Table 3.4

Comparison of % polarisation loss and internal bias values for $+P_r$: S.C. and $+P_r$: N.S.C. in nitrogen and oxygen annealed samples.

	$+P_r$: S.C.			$+P_r$: N.S.C.		
Sample Type	E_i in Kv/cm (Initial)	E_i in Kv/cm (Final)	% Polarization loss	E_i in Kv/cm (Initial)	Ei in Kv/cm (Final)	% Polarization loss
Lirf (N_2 1hr)	-4.85	1.32	52.7	-4.41	-5.74	26.34
Lirf (O_2 1hr)	-20.0	6.0	167.85	-20.0	-20.0	182.14
Lirf (N_2 6hr)	-2.21	3.97	12.44	-3.09	-6.62	14.93
Hirf (N_2 1hr)	-6.32	-4.92	103.42	-11.94	-12.65	6.64
Hirf (O_2 1hr)	7.5	8.75	36.62	-13.75	-23.12	21.08

3.6 Discussion

Our principal motivation in this work has been to evaluate the influences on the electrical properties of PZT thin films due to varying combinations of two processing conditions viz. i) the ambient during annealing and ii) the temperature of the intermediate firing stage. To aid further discussion to our results, it is helpful to recall the nomenclature of the samples according to the combination of processing conditions. This is shown in matrix form below.

	Low Intermediate Firing Temperature (400 ^{0}C)	High Intermediate Firing Temperature (600 ^{0}C)
N_2 Ambient During Annealing	LIRF (1hr, N_2) LIRF (6hr, N_2)	HIRF (1hr, N_2)
O_2 Ambient During Annealing	LIRF (1hr, O_2)	HIRF (1hr, O_2)

It has been recognized earlier [23] that use of nitrogen ambient helps crystallization of PZT thin films into the desired perovskite phase on the basis of comparison between X-ray studies of LIRF (N_2) and LIRF (O_2) films. Our results confirms this conclusion. We note that increasing the annealing time from 1hr to 6hr in N_2 ambient leads to progressive sharpening of PZT related peaks. Majumder et al [23] had attributed better crystallization in N_2 ambient to lesser loss of lead in comparison to O_2 ambient during annealing. In HIRF

films since the crystallization is initiated at the firing stage itself the effect of ambient is not seen.

The leakage current in these films is due to mobile carriers whose concentration depends on the presence of charged defects. For the films annealed in oxygen ambient, it has been observed by Majumder [9], that the leakage current is less for low intermediate rapid firing temperature. This was attributed to a decrease in carrier concentration due to decrease in charged oxygen vacancies in LIRF film. From frequency dependence dielectric dispersion, they argued that the decrease in oxygen vacancies must be due to its complex formation with other positively charged species. However, a similar comparison of leakage current for HIRF and LIRF samples in nitrogen ambient had shown us the reverse i.e. LIRF (N_2) samples have larger leakage current than that of HIRF (N_2) samples. Both the types of samples are expected to have large concentration of oxygen vacancies. However the samples annealed at higher temperature would also have relatively larger number of lead vacancies than its LIRF counterpart. This leads to pair formation by lead and oxygen vacancies to a great extent in HIRF (N_2) films. In LIRF films, since there is more abundance of charged oxygen vacancies even after complex formation with low amount of lead vacancies, the mobile carrier concentration is large. There is a manifestation of similar correlation in depolarization and internal bias measurements which is discussed later in this section. The comparison of leakage currents in LIRF (N_2) and LIRF (O_2) has shown that samples annealed in nitrogen ambient has larger leakage current. This is only to be expected since nitrogen annealed films are expected to have larger oxygen vacancies and hence larger carrier concentration responsible for leakage current. In fact, this can be treated as evidence for the fact that oxygen vacancy concentration is primarily responsible for control of conductivity in PZT thin films.

As regards P-E hysteresis loop measurements, our results show dramatic improvement in properties for sample annealed in N_2 ambient. This has been earlier noted, though not to the same extent, by Chikarmane et al [8] and Majumder [9] in sol-gel derived thin films. There can be almost two fold increase in remnant polarization (P_r) values accompanied by a

similar decrease in value of coercive field (E_c). This indicates that in nitrogen annealed films large degree of domain alignment and easier switching of domains is possible. This can be directly related to increased number of oxygen vacancy concentration in the nitrogen annealed samples. Jaffe [27] has noted that presence of oxygen vacancies make domain movement easier. The slim loop and low dissipation obtained for nitrogen annealed samples amply bear this out. Our results constitute a strong proof of correlation between annealing ambient, concentration of oxygen vacancies and consequent changes in hysteresis parameters. However this tremendous improvement in properties is tempered by the fact that the samples have extremely poor resistance to fatigue. This again reinforces the correlation of fatigue mechanism to concentration of mobile oxygen vacancies. Though there have been controversy regarding exact nature of fatigue mechanism [14, 28, 29], there has been unanimity on the fact that oxygen vacancies are responsible for it. Our results show that the ac properties such as fatigue get affected more severely than do dc leakage currents. This indicates that repeated oxygen vacancy movement across the sample leads to damage resulting in polarization loss and eventually developing electric short.

It is the depolarization behaviour or short time retention properties which is least understood. Mihara et al [12] had initially attributed it to voltage due to external capacitor in a circuit. Later it was argued that the capacitor responsible is internal to the sample in the form of interfacial paraelectric layer. Recently there has been suggestion that depolarization is due to defect dipole in the sample [13]. Previous studies in similar sample in oxygen annealing environment had shown that (i) the depolarization field is constant in its magnitude during the course of depolarization, (ii) the depolarizing field can be changed by external electric field and (iii) that the source of depolarizing field is internal to the sample. Since these are also the characteristic of internal bias, correlation between internal bias and depolarization was suggested. It was also suggested that the internal depolarizing bias may be arising due to space charge created by dipole complexes such as between oxygen vacancy and lead vacancy.

A through-going comparison of depolarization results in differently processed samples can be of considerable help in understanding possible mechanism leading to it. The sample annealed in nitrogen with low intermediate firing temperature, i.e. LIRF (N_2) showed minimum bias values of all the samples studied. This clearly indicates that presence of oxygen vacancies alone is not responsible for internal bias. It is also to be noted that LIRF (N_2) samples are expected to have the least amounts of lead vacancies (V_{pb}''). If formation of dipole complexes are to be regarded as the source of internal bias, then lead vacancies would control the rate limiting step leading to their formation. The percentage of polarization loss in LIRF (N_2) sample is significantly smaller than oxygen annealed samples. This reinferes the idea that source of depolarization also is controlled by the involvement of lead vacancies, most likely through internal bias itself.

The most convincing argument in support of dipole complex involving lead and oxygen vacancies controlling both internal bias and depolarization comes from the results on high intermediate temperature rapid fired samples and annealed in nitrogen ambient i.e. HIRF (N_2) samples. It is this case that we expect large amount of both lead vacancies and oxygen vacancies. In contrast to all other cases, here we obtain a large internal bias of E_i = -20 Kv/cm. Note that it is always negative irrespective of the final polarization and sequence of applied electric field. This indicates that dipole formation is so large that internal bias arising out of this in the space-charge region cannot be switched by the applied external field. The sign of internal bias makes $+P_r$ state as the preferred stable state i.e. the dipolar space charge aids this state of polarization. Significantly in the case of $+P_r$ state, the depolarization in the sample is negligible. However, the depolarization is high when the final state is $-P_r$. This clearly shows that dipole formation is responsible for internal bias, which in turn causes depolarization. Recall that these samples also show lower leakage current due to dipole complex formation.

For HIRF samples annealed in oxygen ambient, the concentration of oxygen vacancies is not so large and hence the formation of $V_{pb}'' - V_o^{\cdot\cdot}$ (in Kroger-Vink notation) complexes are not in such large concentration in space charge region. However they do give rise to

internal bias whose sign depends on the final polarization state of the sample as has been observed for all samples annealed in oxygen ambient irrespective of switching or non-switching of the internal polarization.

In the case of LIRF (O_2) samples, the sample quality is governed by imperfect crystallization and pyrochloro phase formation. The electrical study of these samples have been difficult since they develop electrical shorts quite easily. However for those cases for which results have been reported through earlier studies in our laboratory. The results are consistent with the scheme proposed here. Specifically lower concentration of oxygen vacancies give rise to lower conductivity but the effect of lead vacancies can be appreciable giving in rise to switchable internal bias and depolarization.

There have been earlier studies in similar perovskite systems wherein defect dipoles has been involved to explain internal bias and aging, specially in doped PZT, Barium titanate [30] and PLZT [31] systems. However, defect dipoles alone would not give rise to a constant depolarizing field. Hence Ramesh [13] had suggested a space charge region where the defect associates act as traps and hence control the depolarization field.

High temperature processing involved in the preparation of samples is a known source of oxygen vacancies. This also leads to lead deficiency through PbO formation and its eventual release from the sample. In nitrogen ambient processing conditions, lack of oxygen is obvious. However increase of oxygen vacancy concentration does not leads to concurrent loss of lead from the sample. Hence lead loss is less in nitrogen annealed samples giving rise to comparatively less formation of defects associates involving oxygen vacancy and lead vacancy.

The effect of increased oxygen vacancies concentration leads to

i. easier domain switching resulting in better ferroelectric properties such as larger remnant polarization and lower coercive field

ii. increase in carrier concentration and hence to large leakage current

iii. decrease in fatigue resistance due to damage created by drifting mobile oxygen vacancies

On the other hand lead vacancies form defect dipoles or associates with oxygen vacancies leading to

i. removal of charged oxygen vacancies and hence to lower conductivity

ii. strong internal bias through their presence in space charge layers

iii. source of depolarization through internal bias in the absence of any external field

Hence our results indicate that processing conditions make their impact on electrical properties mainly through oxygen vacancies and lead vacancies. Nitrogen ambient annealing increases oxygen vacancies concentration and high temperature annealing increases lead vacancy concentration.

Though, in this work the dramatic increase in ferroelectric properties were found to be at the cost of unacceptable level of fatigue resistance, the understanding gained would be of help in optimizing process conditions. For example, one can proceed to design processing conditions with acceptable trade-off between the two by suitable doping. Majumder et al [26] have recently shown that an isovalence dopant such as Cerium in PZT binds oxygen vacancies and improve fatigue resistance. Rendering oxygen vacancies immobile would improve fatigue resistance but their presence in the bulk could still help easier switching and hence better ferroelectric properties.

In summary, we have evaluated the influence of ambient during annealing on the electrical properties of sol-gel derived PZT thin films. We have obtained correlations between combination of ambient and heating schedule during processing with properties such as the dc leakage current, ferroelectric hysteresis loop parameters, fatigue resistance and short time depolarization characteristics. It has been shown that it is possible to rationalize all the observations qualitatively through the effect that these processing

conditions have on the concentration of oxygen vacancy and lead vacancy. The free oxygen vacancy concentration controls conductivity and fatigue resistance. Increased probability of formation of lead vacancy controls hysteresis loop parameter and depolarization characteristic.

Chapter 4

Summary and Conclusions

Thin films of ferroelectric lead zirconate titanate (PZT) have many potential applications including that of non-volatile random access memory in computer systems. However, there are at present several problems relating to the electrical properties of these films such as fatigue, depolarization and imprint which are not well understood. In literature few reports have appeared on the effect of ambient on the electrical properties of the films. The exact role of vacancies on the properties of the films are not well understood. In this work the properties of nitrogen annealed films are studied and compared with oxygen annealed films to evaluate the role of combination of ambient and heating schedules on the electrical properties viz. dc leakage current, hysteresis loop parameters and depolarization characteristics. Special emphasis is given to depolarization study of the films.

Crack free films of $Pb_{1.05}(Zr_{0.53}Ti_{0.47})O_3$ with thickness in the range of 1.7-1.78μm have been prepared using modified sol-gel technique on Pt substrates. For studying the effect of ambient on final stage of annealing two different heat treatment sequences were used. In all samples nitrogen was used as the ambient during the final stage of annealing. Those sample which are fired at 400 ^{0}C during intermediate stage and annealed at 700 ^{0}C are termed as LIRF samples. Those fired at 600 ^{0}C and annealed at 700 ^{0}C are termed as HIRF samples.

Routine characterization of samples has been carried out using several techniques including Double Beam Spectrophotometry to obtain film thickness, XRD to study the phase formation, I-V measurements for leakage current, and P-E hysteresis measurements to study the ferroelectric nature of the films.

The depolarization behaviour of PZT thin films has been studied using a new measurement sequence which consists of following steps: I) Polarize the sample to the desired polarization state utilizing the P-E measurements ii) Switching or reinforcing the polarization state by applying a square voltage pulse and iii) monitoring the remnant polarization as a function of time. P-E measurements have been carried out at various steps to observe the possible changes in the loop parameters. Some of the significant observations and conclusions of this work are listed below.

1. Perovskite phase was obtained for all the samples studied. However, peaks in the spectra for LIRF (N_2) are broader than those for LIRF (O_2) which indicates that perovskite phase formation is slower in nitrogen ambient than oxygen ambient. Again the peaks of LIRF (6Hr N_2) are sharper than LIRF (1Hr N_2) samples. So with increase in annealing time, peaks corresponding to the perovskite phase become progressively sharper. However for samples fired at high intermediate temperature, ambient has no significant effect on phase formation.
2. The samples annealed in nitrogen ambient have significantly higher remnant polarization and lower coercive field than those annealed in oxygen. This improvement in ferroelectric parameter attributed to presence of oxygen vacancies which make domain movement easier.
3. For nitrogen ambient annealing, sample fired at low intermediate temperature have larger leakage current than its oxygen annealed counterpart. On the other hand keeping the heating schedule same as HIRF, oxygen ambient annealed sample have higher leakage current. Both the observations are consistent with the fact that concentration of free charged oxygen vacancies control conductivity. When lead vacancies and oxygen vacancies are in large concentration, the leakage current get reduced due to pair formation between lead and oxygen vacancies.
4. All nitrogen annealed samples have poor fatigue characteristics due to presence of large number of oxygen vacancies.
5. During depolarization measurements in LIRF(N_2) samples there is a strong correlation between the final polarization state achieved and the final internal bias. If the final

polarization state achieved is $+P_r$ then internal bias is negative and vice versa, whereas for HIRF(N_2) sample, the internal bias is found to be always negative indicating that positive polarization state is the preferred stable state.

6. The polarization loss percent in LIRF(N_2) samples are lower than LIRF(O_2) samples. This correlates with the occurrence of lower internal bias in LIRF(N_2) samples than LIRF(O_2) samples.
7. Polarization loss is found to be smaller in all cases of nitrogen annealed samples except for HIRF (N_2) samples. For HIRF (N_2) samples, polarization loss is found to be high only when the polarization state is switched from positive remnant polarization to negative remnant polarization. This observation provides proof of the fact that internal bias is responsible for depolarization.
8. The experimental observations are correlated with processing conditions through a comparison of measured properties for different combinations of ambient and heating schedule. It is found that nitrogen annealing ambient, leads to large concentration of oxygen vacancies which in turn leads to i) larger leakage current, ii) easier domain switching, and iii) poorer fatigue resistance.
9. It is concluded that annealing under oxygen ambient and at high temperature favour formation of lead vacancies. These lead vacancies tend to form defect dipoles or associates with oxygen vacancies leading to i) removal of charged oxygen vacancies and hence to lower conductivity, ii) strong internal bias through their presence in space charge layers, and iii) source of depolarization through internal bias in the absence of any external field.

In summary, we have evaluated the influence of ambient during annealing on the electrical properties of sol-gel derived PZT thin films. We have obtained correlation between combination of ambient and heating schedule during processing with properties such as the dc leakage current, ferroelectric hysteresis loop parameters, fatigue resistance and short time depolarization characteristics. It has been shown that it is possible to rationalize all the observations quantitatively through the effect that these processing

conditions have on the concentration of oxygen vacancy and lead vacancy. The free oxygen vacancy concentration controls conductivity and fatigue resistance. Increased probability of formation of lead vacancy controls hysteresis loop parameter and depolarization characteristic.

4.1 Scope For Future Work

On the basis of our studies, we suggest the following as obvious extension of this work:

I. The optimum level of oxygen vacancies required to obtain a trade-off between fatigue resistance and ferroelectric properties is needed. This could be achieved by studying a further variation in processing parameters.

II. PZT films with suitable dopants, such as isovalence Cerium, can be used to render oxygen vacancies immobile improving fatigue resistance.

III. The nature of defect complexes formed during such processing need to be studied in more detail specifically through frequency dependence dielectric studies.

IV. The correlation between internal bias and depolarization needs to be quantified by making fast hysteresis loop measurements.

Bibliography

[1] C. Feldman, *Rev. Sci. Instr.*, **26**, 463 (1955)

[2] A. Moll, *Z. Angew. Phys.*, **10**, 463 (1958)

[3] E. K. Muller, B. J. Nicholson, and G. E. Turner, *J. Electrochem. Soc.*,**110**, 969 (1963)

[4] J. F. Scott, L. Kammerdiner, M. Paris, S. Traynor, V. Ottenbacher, A. Shawabkeh, and W. F. Oliver, *J. Appl. Phys.*, **64**, 787 (1988)

[5] J. F. Scott and C. A. Paz de Araujo, *Science*, **246**, 1400 (1989)

[6] T. Mihira, H. Watanabe, and C. A .P. Araujo, *Jpn. J. Appl. Phys.*, **33**, 3996 (1994)

[7] Tkahashi Mihira, Hiroyuki Yoshimori, Hitoshi Watanabe, and Carlos A. Pazde Araujo, *Jpn. J. Appl. Phys.*, **34**, 2380 (1995)

[8] Vinay Chikarmane, Chandra Sudhama, Jiyoung Kim, Jack Lee, Al Tasch, and Steve Novak, *J. Vac. Sci. Technol.*, **A 10(4)**, 1562, (1992)

[9] Subasish Basu Majumder, *Ph. D. Thesis*, Submitted to the Mat. Sci. Prog., I. I. T. Kanpur, India, March, 1997

[10] J. M. Benedetto, R. A. Moore, and F. B. McLean, *J. Appl. Phys.*, **75**, 460 (1994)

[11] A. M. Lines and Glass, *Principles and applications of ferroelectrics and related meterials*, Clarendon Press, Oxford, 1997

[12] T. Mihara, H. Watanabe, and C. A. Araujo, *Jpn. J. Appl. Phys.*, **32**, 4168 (1993)

[13] V. Ramesh, *M. Tech. Thesis*, Materials Science Programme, I.I.T. Kanpur, (1996)

[14] J. F. Scott, C. A. Araujo, B. M. Melnick, L. D. McMillan, and R. Zuleeg, *J. Appl. Phys.*, **70**, 382 (1991)

[15] T. Hase and T. Shiosaki, *Jpn. J. Appl. Phys.*, **30**, 2159 (1991)

[16] T. Katayama, M. Sugiyama, M. Shimizu, and T. Shiosaki, *Jpn. J. Appl. Phys.*, **31**, 3005 (1992)

[17] H. Kidoh, T. Ogawa, H. Yashima, A. Morimoto, and T. Shimizu, *Jpn. J. Appl. Phys.*, **31**, 2965 (1992)

[18] Chi. Kwok, S. B. Desu, and D. P. Vijay, *Ferroelectric Letters*, **116**, 143 (1994)

[19] M. Mayer, *Con. Ceram. Quart*, **21**, 59 (1990)

[20] R. C. Mehrotra, *J. Non. Cryst. Solids*, **121**, 1 (1990)

[21] Guanghua Yi and Michael Sayer, *Ceramic Bulletin*, **70**, 1773 (1991)

[22] R. Schwartz, B. Bunker, D. Dimos, R. Assink, and D. Tallantandi, *Ferroelectrics*, 1991

[23] S. B. Majumder, D. C. Agarwal, Y. N. Mohapatra, and V. N. Kulkarni, *Integrated ferroelectrics*, **9**, 271 (1995)

[24] C. B. Sawyer and C. H. Tower, *Physical Review*, **35**, 269 (1930)

[25] S. K. Dey, J. J. Lee and P. Alluri, *Jpn. J. Appl. Phys.*, **34**, 3142 (1995)

[26] S. B. Majumder, Y. N. Mohapatra, and D. C. Agrawal, *Appl. Phys. Lett.*, **69**, Dec (1996)

[27] B. Jaffe, *Piezoelectric Ceramics*, Academic Press London, 1971

[28] J. J. Lee, C. L. Thio, and S. B. Desu, *J. Appl. Phys.*, **78**, 5073 (1995)

[29] W. L. Warren, D. Demos, B. A. Tuttle, R. D. Nasby, and G. E. Pike, *Appl. Phys. Lett.*, **65**, 1018 (1994)

[30] R. Lohkamper, H. Neumann, and G. Arlt, *J. Appl. Phys.*, **68**. 4220 (1990)

[31] G. E. Pike, W. L. Warren, D. Dimos, B. A. Tuttle, R. Ramesh, J. Lee, V. G. Keramidas, and J. T. Evan, *Appl. Phys. Letter,* **66**, 484 (1995)